Anticancer Chemotherapy Inhibits MHC Class I–Related Chain A Ectodomain Shedding by Downregulating ADAM10 Expression in Hepatocellular Carcinoma

Keisuke Kohga, Tetsuo Takehara, Tomohide Tatsumi, Takuya Miyagi, Hisashi Ishida, Kazuyoshi Ohkawa, Tatsuya Kanto, Naoki Hiramatsu, and Norio Hayashi

Department of Gastroenterology and Hepatology, Osaka University Graduate School of Medicine, Osaka, Japan

Abstract

MHC class I–related chain A (MICA) is a ligand for the NKG2D-activating immunoreceptor that mediates activation of natural killer (NK) cells. The ectodomain of MICA is shed from tumor cells, which may be an important means of evading antitumor immunity. We previously reported that patients with hepatocellular carcinoma (HCC) display high levels of soluble MICA in circulation, which could be downregulated by chemotherapy. The present study shows that anti-HCC drugs suppress MICA ectodomain shedding by inhibiting expression of a disintegrin and metalloproteinase 10 (ADAM10). Both ADAM10 and CD44, a typical substrate of the ADAM10 protease, were expressed in human HCC tissues and HCC cells but not in normal liver tissues or cultured hepatocytes. Small interfering RNA–mediated knockdown experiments revealed that ADAM10 is a critical sheddase for both MICA and CD44 in HCC cells. Of interest is the finding that epirubicin clearly downregulated ADAM10 expression and MICA shedding in HCC cells; its suppressive effect on MICA shedding was abolished in ADAM10-depleted cells. Epirubicin treatment also enhanced the NKG2D-mediated NK sensitivity of HCC cells. Patients with HCC had significantly higher levels of serum-soluble CD44, which correlated well with serum-soluble MICA levels, thus suggesting a close link between ADAM10 activity and MICA shedding in these patients. Soluble MICA and CD44 levels were downregulated with a significant correlation in patients treated by transarterial chemoembolization using epirubicin. In conclusion, anticancer drugs can modulate expression of ADAM10, which is critically involved in MICA ectodomain shedding. Epirubicin therapy may have a previously unrecognized effect on antitumor immunity in HCC patients. [Cancer Res 2009;69(20):8050–7]

Introduction

Hepatocellular carcinoma (HCC) is one of the leading causes of cancer deaths worldwide. Chronic liver disease caused by hepatitis virus infection and nonalcoholic steatohepatitis leads to a predisposition for HCC, with liver cirrhosis, in particular, being considered a premalignant condition (1, 2). With regard to treatment, surgical resection or percutaneous techniques such as ethanol injection and radiofrequency ablation are considered to be choices for curable treatment of localized HCC, whereas transcatheter arterial chemoembolization (TACE) is a well-established technique for more advanced HCC (3). The liver contains a large compartment of innate immune cells [natural killer (NK) cells and natural killer T cells] and acquired immune cells (T cells; refs. 4, 5), but the activation of these immune cells after HCC treatments remains unclear. If such treatments can efficiently activate abundant immune cells in the liver, this could lead to the establishment of attractive new strategies for HCC treatment.

MHC class I–related chain A and B (MICA and MICB) are ligands for NKG2D expressed on a variety of immune cells (6). In contrast to classic MHC class I molecules, MICA/B are rarely expressed on normal cells but frequently on tumor cells (7–10). The engagement of MICA/B and NKG2D strongly activates NK cells and costimulates T cells, enhancing their cytolytic activity and cytokine production (11). Thus, the MICA/B-NKG2D pathway is an important mechanism by which the host immune system recognizes and kills transformed cells (12). In addition to those membrane-bound forms, MICA/B molecules are also cleaved proteolytically from tumor cells and appear as soluble forms in sera of patients with malignancy (13–15). Soluble MICA/B in circulation downregulates NKG2D expression and disturbs NKG2D-mediated antitumor immunity (9, 10, 13). We previously reported that soluble MICA could be detected in sera of HCC patients (16) and that TACE treatment reduces the levels of soluble MICA and thereby upregulates the expression of NKG2D (17). Thus, cancer therapy may have a beneficial effect on NKG2D-mediated immune responses.

The release of soluble MICA/B from tumor cells is impaired by metalloproteinase inhibitors, suggesting the involvement of members of the metzincin superfamily, such as ADAM proteins (14, 18). In addition, ERp5, related to protein disulfide isomerase, is required for the MICA shedding as it reduces disulfide bond of the α3 domain of MICA (19). Although it may not be a direct protease for MICA, it may enable proteolytic cleavage through conformational change. Recently, it was reported that MICA shedding of 293T fibroblast cells and HeLa cervical cancer cells was inhibited by silencing of the ADAM10 and ADAM17 proteases (20). This suggests that ADAM family proteins may be a therapeutic target for enhancing antitumor immunity, but how to therapeutically modulate these proteins is still not clear. Furthermore, it remains to be determined whether ADAMs can regulate MICA shedding in a clinical setting.

In the present study, we showed that ADAM10, but not ADAM17, was critically required for MICA shedding in human HCC cells. Of importance is the discovery that epirubicin, a widely used anti-HCC drug, was capable of downregulating ADAM10 expression and

Note: Supplementary data for this article are available at Cancer Research Online (http://cancerres.aacrjournals.org/).

K. Kohga, T. Takehara, and T. Tatsumi contributed equally to this work.

Requests for reprints: Norio Hayashi, Department of Gastroenterology and Hepatology, Osaka University Graduate School of Medicine, 2-2 Yamadaoka, Suita, Osaka 565-0871, Japan. Phone: 81-6-6879-3621; Fax: 81-6-6879-3629; E-mail: hayashin@gh.med.osaka-u.ac.jp.

doi:10.1158/0008-5472.CAN-09-0789

activity in HCC cells; it can thus inhibit MICA shedding and enhance NK sensitivity. ADAM10 was immunohistochemically detected in HCC tissues and a correlation was observed between soluble MICA levels and ADAM10 activity determined by soluble CD44 levels in HCC patients. The present study sheds light on previously unrecognized effects of an anticancer drug on modulating ADAM family proteins and MICA shedding and thus suggests a promising aspect for chemoimmunotherapy against human HCC.

Materials and Methods

Liver tissues and immunohistochemistry. Human HCC tissues (n = 8) and normal liver tissues (n = 2) obtained at surgical resection were used. Informed consent, under an institutional review board–approved protocol,

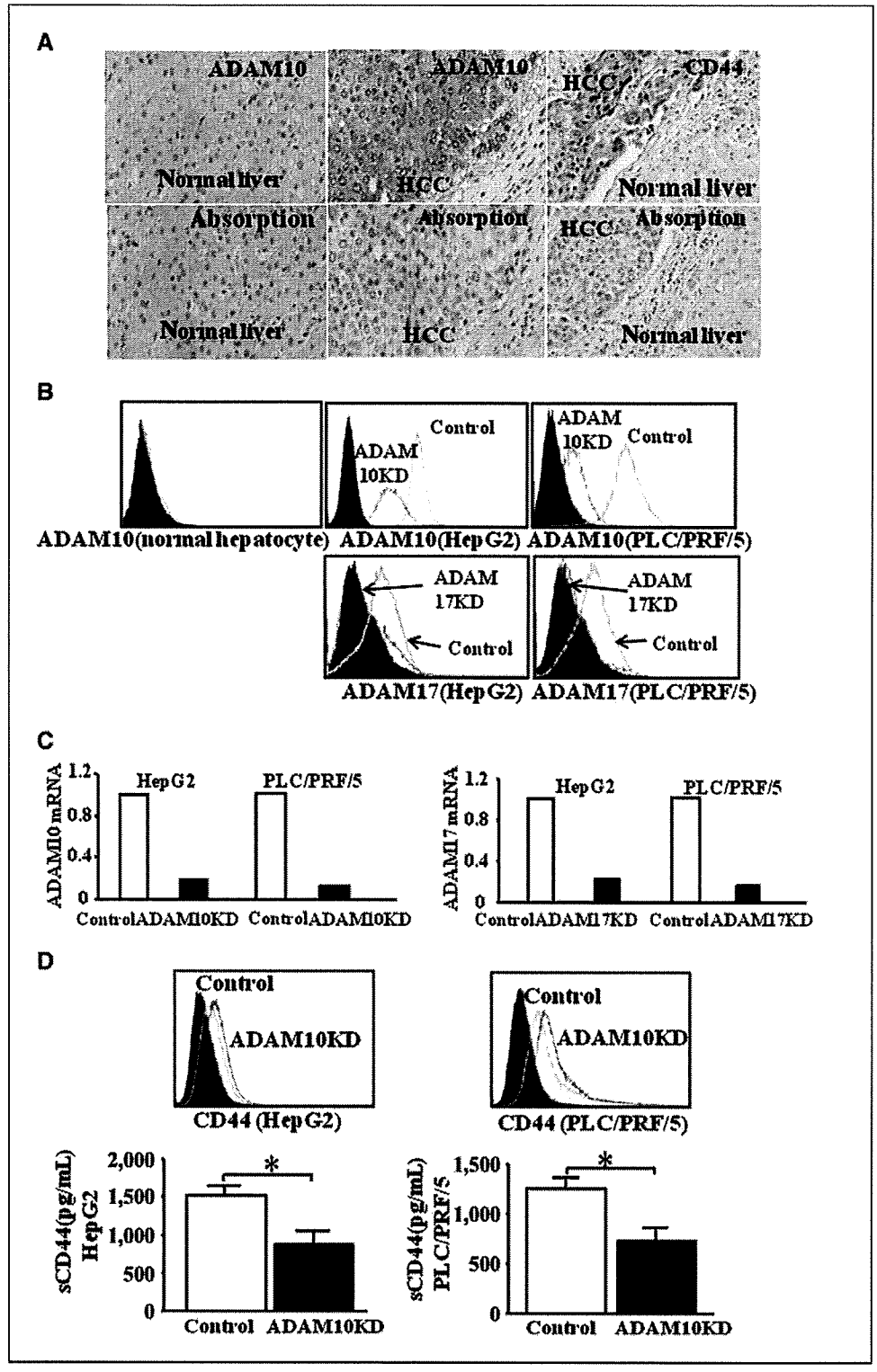

Figure 1. Expression of ADAM10 and CD44 in human HCC tissues and ADAM10 or ADAM17 knockdown in human HCC cells. *A*, immunohistochemical detection of ADAM10 and CD44 in human HCC tissues (n = 8) and normal liver tissues (n = 2). Liver sections were stained with the corresponding antibodies (*top panels*). Both primary antibodies were incubated with recombinant CD44 and ADAM10 proteins and then applied to liver sections in parallel as the absorption test (*bottom panels*). Representative images are shown. *B* and *C*, expression of ADAM10 or ADAM17 in human primary hepatocyte and HCC cell lines (*HepG2* and *PLC/PRF/5*). Cells were treated with ADAM10 siRNA, ADAM17 siRNA, or control siRNA, and subjected to analysis of ADAM10 or ADAM17 expression by flow cytometry (*B*) or real-time RT-PCR (*C*). *Histograms*, anti-ADAM10 or anti-ADAM17 staining of ADAM10 or ADAM17 siRNA-treated cells (*ADAM10KD* or *ADAM17KD, black dotted line*) and control siRNA-treated cells (*Control, gray line*), respectively. *Closed histograms*, control IgG staining. *D*, the expression of membrane-bound CD44 on HCC cells treated with ADAM10 siRNA (ADAM10KD, *black line*) or control siRNA (*Control, gray line*) was evaluated by flow cytometry (*top panels*). *Closed histograms*, control IgG staining. Soluble CD44 (*sCD44*) production from HCC cells treated with ADAM10 siRNA or control siRNA were evaluated by specific ELISA (*bottom panels*). *, $P < 0.05$.

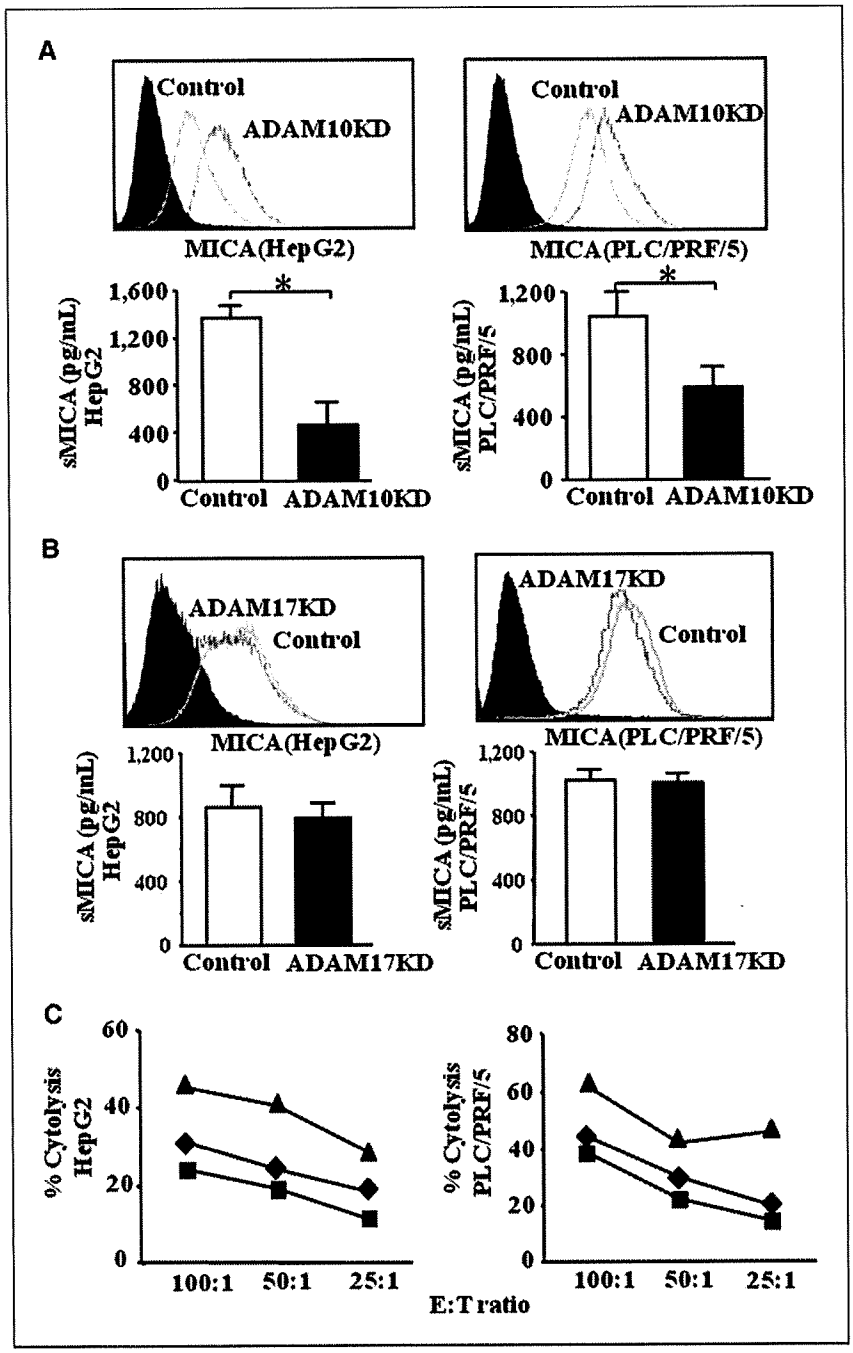

Figure 2. Expression of MICA in ADAM10 or ADAM17 knockdown HCC cells and NK sensitivity in ADAM10 knockdown HCC cells. *A* and *B*, the expression of membrane-bound MICA on HCC cells treated with ADAM10 siRNA (*ADAM10KD, black line*; *A*), ADAM17 siRNA (*ADAM17KD, black line*; *B*), or control siRNA (*Control, gray line*) was evaluated by flow cytometry (*top panels*). *Closed histograms*, control IgG staining. Soluble MICA (*sMICA*) production from HCC cells treated with ADAM10 siRNA (*A*), ADAM17 siRNA (*B*), or control siRNA were evaluated by specific ELISA (*bottom panels*). *, $P < 0.05$. *C*, HCC cells treated with ADAM10 siRNA or control siRNA were subjected to ^{51}Cr-release assay against NK cells. Cytolytic activity of NK cells against control HCC cells (■) or ADAM10 knockdown HCC cells without (▲) or with blocking antibody of MICA/B (6D4; ♦). Representative results are shown. Similar results were obtained from three independent experiments.

was obtained from all patients before sample acquisition. Liver sections were subjected to immunohistochemical staining using the ABC procedure (Vector Laboratories, Burlingame, CA). The primary antibodies used were anti-ADAM10 and anti-CD44 (R&D Systems). To confirm the specificity of the staining, primary antibodies were incubated with recombinant CD44 or ADAM10 protein (R&D Systems, Minneapolis, MN) for 3 h and then applied onto liver sections in parallel with staining of the primary antibodies as the absorption test.

HCC cell lines. Human HCC cell lines HepG2 and PLC/PRF/5 were purchased from the American Type Culture Collection and were cultured with DMEM supplemented with 10% fetal bovine serum (GIBCO/Life Technologies, Grand Island, NY) in a humidified incubator at 5% CO_2 and 37°C.

RNA silencing. The small interfering RNA (siRNA) method was used to knockdown ADAM10 and ADAM17. Stealth RNAi oligonucleotide targeting ADAM10 or ADAM17 and scrambled oligonucleotides as a control were purchased from Invitrogen (Carlsbad, CA). Cells were transfected by RNAi Max transfection reagent (Invitrogen) with 50 nmol/L siRNA. At 24 h posttransfection, the cells were analyzed for specific depletion of the mRNAs of ADAM10 and ADAM17 by real-time reverse transcription-PCR (RT-PCR; Applied Biosystems, Foster City, CA). The following siRNAs were used: ADAM10, 5′-AUAUCUGGGCAAUCACAG-CUUCUCG-3′; scramble control, 5′-AUACUUGGUCAACGCACUUCGAUGG-3′; ADAM17, 5′-UGAACAAGCUCUUCAGGUGGUUCUC-3′; scramble control, 5′-UGAUUAGAACUCUCGACUGGUGCUC-3′.

ELISA. The supernatants of cultured cells were harvested at 24 h after transfection with siRNA as well as sera from HCC patients ($n = 97$) and age-matched healthy volunteers ($n = 32$) were subjected to analysis of soluble MICA and soluble CD44 levels. Informed consent, under an institutional review board–approved protocol, was obtained from all patients before sample acquisition. The levels of soluble MICA and soluble CD44 were

determined by DuoSet MICA eELISA kit (R&D Systems) and soluble CD44std ELISA (Abcam, Cambridge, MA), respectively.

Flow cytometry. For the detection of membrane-bound MICA and CD44, cells were incubated with an anti-MICA–specific antibody (2C10, Santa Cruz Biotechnology, Santa Cruz, CA) or anti-CD44 antibody (R&D Systems) and stained with phycoerythrin (PE)-goat anti-mouse immunoglobulin (Beckman Coulter) as a secondary reagent and then subjected to flow cytometric analysis. For the detection of ADAM10 or ADAM17, cells were fixed and permeabilized with Cytofix/Cytoperm (BD Biosciences, San Jose, CA) and stained with PE-conjugated anti-ADAM10 or anti-ADAM17 antibody (R&D Systems). Flow cytometric analysis was performed using a FACScan flow cytometer (Becton Dickinson).

Plasmid construction of pMyc-MICA. MICA full coding cDNA was isolated from Huh7, human HCC cells, using a conventional RT-PCR method (Supplementary Fig. S1, DDBJ/EMBL/Genbank accession number AB506764) and inserted into the *Hin*dIII-*Xba*I site of pcDNA3 (Invitrogen). A C-myc tag was placed between the leader peptide and the α1 domain of MICA by site-specific mutagenesis using a QuikChange site-directed mutagenesis kit (Stratagene, La Jolla, CA) referred to as pMyc-MICA. Cells were transfected with pMyc-MICA using a Lipofectamine LTX reagent (Invitrogen). The green fluorescent protein (GFP)–expressing vector (pEGFP-C1, Clontech, Mountain View, CA) was cotransfected to evaluate the transfection efficiency.

Immunoprecipitation. Cells or tissues were homogenized in lysis buffer containing 1% NP40, 0.5% sodium deoxycholate, 0.1% SDS, 50 μg/mL aprotinin, 100 μg/mL phenylmethylsulfonyl fluoride, 1 mmol/L sodium orthovanadate, 50 mmol/L sodium fluoride, and PBS. To the cell supernatants, 0.5% NP40 and a cocktail of protease inhibitors were added. The protein contents of the samples were determined by BCA protein assay kit (Pierce, Rackford, IL). Immunoprecipitation with anti–c-Myc beads was performed for 1 h at 4°C. Immunocomplexes were eluted by a c-Myc–tagged peptide solution (MBL, Woburn, MA). The samples after immunoprecipitation were treated with 250 mU of N-glycosidase F (Roche, Mannheim, Germany) for 3 h at 37°C.

Western blotting. The total cellular protein was electrophoretically separated using SDS-12% polyacrylamide gels and transferred onto polyvinylidene difluoride membrane. The membrane was blocked in TBS-Tween containing 5% skim milk for 1 h and then probed with anti-Myc mouse monoclonal antibody (Cell Signaling Technology, Danvers, MA) at 4°C overnight. Horseradish peroxidase–conjugated anti-rabbit antibody and SuperSignal West Pico System (Pierce) were used for the detection of blots.

Real-time RT-PCR. Total RNA was isolated using RNeasy Mini Kit (Qiagen K.K., Tokyo, Japan) and was reverse transcribed using SuperScript III First-Strand Synthesis System (Invitrogen). The mRNA levels were evaluated using ABI PRISM 7900 Sequence Detection System (Applied Biosystems). Ready-to-use assays (Applied Biosystems) were used for the quantification of ADAM10 (Hs00153853_m1), ADAM17 (Hs00234221_m1), MICA (Hs00792195_m1), β-actin (Hs99999903_m1), and CD44 (Hs00174139_m1) mRNAs according to the manufacturer's instructions. The thermal cycling conditions for all genes were 2 min at 50°C and 10 min at 95°C, followed by 40 cycles at 95°C for 15 s and 60°C for 1 min. β-Actin mRNA from each sample was quantified as an endogenous control of internal RNA.

WST-8 assay. HepG2 and PLC/PRF/5 cells were treated with different concentrations of epirubicin for 24 h. Cell growth of epirubicin-treated HCC cells was determined by WST-8 assay (Nacalai Tesque, Kyoto, Japan) as previously described (21).

NK cell analysis. NK cells were isolated from human peripheral blood mononuclear cells by magnetic cell sorting using CD56 MicroBeads (Miltenyl Biotech, Auburn, CA) as previously described (16). The cytolytic ability of NK cells was assessed by 4-h ^{51}Cr-releasing assay with or without MICA/B-blocking antibody (6D4; ref. 7), which binds to the α1 and α2 domains of MICA and MICB. 6D4 was a generous gift from Drs. Veronika Groh and Thomas Spies (Fred Hutchinson Cancer Research Center, Seattle, WA).

Statistics. All values were expressed as the mean and SD. The statistical significance of differences between the groups was determined by applying Student's *t* test or two-sample *t* test with Welch correction after each group

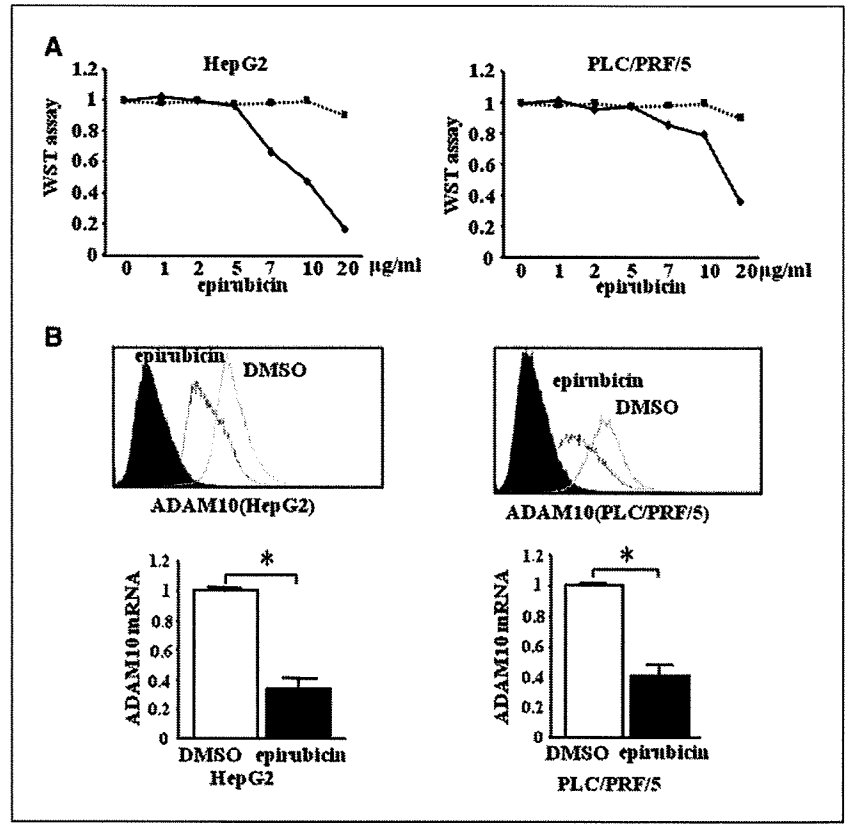

Figure 3. Expression of ADAM10 in epirubicin-treated HCC cells. *A*, the cytotoxicity of epirubicin to human HCC cells was evaluated by WST-8 assay. Cells were treated with different doses of epirubicin (*solid lines*) or vehicle (*DMSO*; *dotted lines*) for 24 h, and the viability of the cells was evaluated by the WST-8 assay. *B*, ADAM10 expression of epirubicin-treated HCC cells. Cells were treated with a nontoxic dose of 1 μg/mL epirubicin (*black lines*) or vehicle (DMSO, *gray lines*) for 24 h and their ADAM10 expression was evaluated by flow cytometry (*top panels*). *Closed histograms*, control IgG staining. Total RNA was extracted at 24 h of epirubicin treatment and mRNA levels of ADAM10 were evaluated by real-time RT-PCR (*bottom panels*). *, $P < 0.05$.

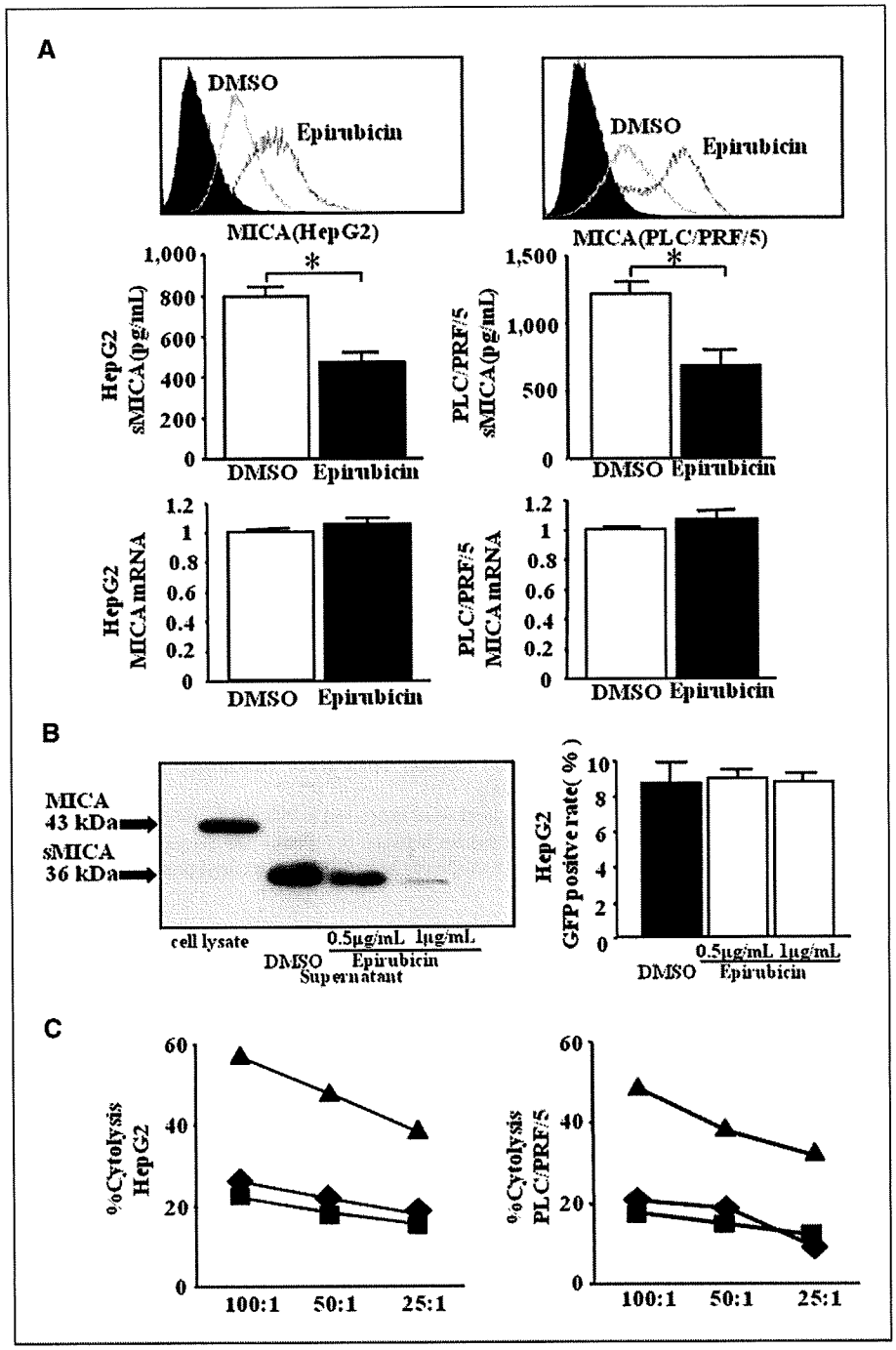

Figure 4. Expression and shedding of MICA in epirubicin-treated HCC cells. *A*, HCC cells were treated with a nontoxic dose of 1 μg/mL epirubicin (*black lines*) or vehicle (DMSO, *gray lines*) for 24 h and their expression of membrane-bound MICA and MICA mRNA was evaluated by flow cytometry (*top panels*) and real-time RT-PCR (*bottom panels*), respectively. *Closed histograms*, control IgG staining in flow cytometry. At the same time, 24-h culture supernatants were subjected to the analysis of soluble MICA (*sMICA*) levels by ELISA (*middle panels*). *, $P < 0.05$. *B*, HepG2 cells were transfected with pMyc-MICA and pEGFP-C1, cultured with 0.5 to 1 μg/mL epirubicin or vehicle (DMSO) for 24 h. Cell lysates from HepG2 cells and 24-h culture supernatants of epirubicin- or vehicle-treated HepG2 cells were immunoprecipitated with anti-Myc. The resulting immunoprecipitates were eluted, treated with N-glycanase, and subjected to Western blot analysis for MICA (*left*). Transfection efficacies were equal in all treatment groups as evidenced by similar GFP-positive cell rates (*right*). *C*, the cytolytic activity of NK cells against HCC cells. Vehicle-treated cells (■) or epirubicin-treated cells without (▲) or with blocking antibody of MICA/B (6D4; ♦) were subjected to ^{51}Cr-release assay. Representative results are shown. Similar results were obtained from three independent experiments.

had been tested with equal variance and Fisher's exact probability test. We defined statistical significance as $P < 0.05$.

Results

ADAM10 and CD44 are overexpressed in human HCC. ADAM10 was detected in all human HCC tissues tested by immunohistochemistry but not in normal liver tissues (Fig. 1*A*). Flow cytometric analysis revealed that ADAM10 was strongly expressed in a variety of HCC cell lines, including HepG2, PLC/PRF/5 (depicted in Fig. 1*B*), and Hep3B (data not shown), but faintly in primary hepatocytes. CD44, a typical substrate of the ADAM10 protease, was also expressed in all human HCC tissues but not in normal liver tissues (Fig. 1*A*). The data suggest that overexpression of ADAM10 and CD44 is a characteristic of human HCC like other malignancies (22).

ADAM10 is involved in MICA shedding of HCC cells but ADAM17 is not. To examine the involvement of ADAM family proteins in MICA ectodomain shedding, ADAM10 or ADAM17 were knocked down in HCC cells using a siRNA-mediated procedure. ADAM10 expression was clearly suppressed in HepG2 cells and PLC/PRF/5 cells at both mRNA and protein levels (Fig. 1*B* and *C*). Both cell lines expressed CD44 on the cellular surface and produced significant levels of soluble CD44 (Fig. 1*D*), indicating that CD44 is expressed and shed from those cell lines. ADAM10 knockdown (KD)

led to an increase in CD44 expression on HCC cells and a decrease in soluble CD44 levels in culture supernatants (Fig. 1*D*). Because ADAM10 has been established as being a sheddase for CD44, siRNA-mediated knockdown of ADAM10 suppressed not only the expression but also the activity of ADAM10 in HCC cells. HepG2 and PLC/PRF/5 cells also expressed ADAM17, which was clearly knocked down by a siRNA-mediated procedure (Fig. 1*B*).

HepG2 cells and PLC/PRF/5 cells expressed membrane-bound MICA and also produced soluble MICA (Fig. 2*A*). Knockdown of ADAM10 for both cell lines clearly upregulated MICA expression on their cellular surface and downregulated soluble MICA levels in their culture supernatant (Fig. 2*A*). In contrast, knockdown of ADAM17 did not affect the expression of membrane-bound MICA or the production of soluble MICA (Fig. 2*B*). We also examined the involvement of ADAM17 in MICA shedding of phorbol 12-myristate 13-acetate (PMA)–stimulated HCC cells because ADAM17 is considered to primarily affect stimulated shedding. The expression of membrane-bound MICA and the soluble MICA production were equal between PMA-stimulated ADAM17KD-HCC cells and control HCC cells (Supplementary Fig. S2). Thus, ADAM10, but not ADAM17, is critically involved in the shedding of MICA in HCC cells.

We next evaluated the cytolytic activity of NK cells against HCC cells. The cytolytic activity of NK cells against ADAM10KD-HepG2 cells was higher than that against control HepG2 cells. This activity was inhibited by blocking of anti-MICA/B antibody, suggesting that the increase of NK sensitivity depended on the increased expression of membrane-bound MICA on ADAM10KD-HepG2 cells, although we could not exclude the possibility of the involvement of MICB in this cytotoxicity (Fig. 2*C*). Similar results were also obtained with ADAM10KD-PLC/PRF/5 cells.

Epirubicin suppresses ADAM10 expression in HCC cells. We examined the biological modification of human HCC cells by adding epirubicin, which is commonly used in anti-HCC chemotherapy. We first examined the cytotoxicity of epirubicin to human HCC cells by WST-8 assay. Adding >5 μg/mL of epirubicin resulted in a significant decrease in cell growth of both HepG2 and PLC/PRF/5 cells (Fig. 3*B*). Based on these findings, we used 1 μg/mL of epirubicin to evaluate the biological effect on human HCC cells without toxicity. Both HepG2 cells and PLC/PRF/5 cells were cultured for 24 h with epirubicin and then subjected to analysis of ADAM10 expression. Epirubicin suppressed ADAM10 expression at the mRNA and protein levels in both cell lines (Fig. 3*C*). Although the data are not shown, doxorubicin also suppressed ADAM10 expression in HCC cells.

Epirubicin inhibits MICA ectodomain shedding and enhances susceptibility to NK cells of HCC cells. The above observations led us to investigate whether epirubicin or doxorubicin treatment would affect MICA ectodomain shedding in HCC cells. Epirubicin treatment led to an increase in membrane-bound MICA expression and a decrease in soluble MICA production in both HepG2 and PLC/PRF/5 cells (Fig. 4*A*). The mRNA levels of MICA did not change after exposure to epirubicin in both HCC cells (Fig. 4*A*). Similar data were obtained with doxorubicin-treated cells (data not shown).

To confirm whether the soluble MICA detected by ELISA was actually reflected in the cleaved form, we transfected Myc-tagged MICA into HepG2 cells and collected culture supernatants as well as cellular lysates. Immunprecipitates from these samples with anti-Myc were subjected to Western blot analysis after treatment with N-glycosidase. MICA in the culture supernatants migrated faster than cellular MICA (Fig. 4*B*), indicating that the MICA detected by ELISA is actually processed and released from full-length MICA. Epirubicin treatment led to a decrease in soluble MICA protein in HepG2 cells (Fig. 4*B*).

We next evaluated whether the epirubicin treatment could also modify the NK sensitivity of human HCC cells. Epirubicin-treated HepG2 cells or PLC/PRF/5 cells were more susceptible to NK cells than nontreated HepG2 or PLC/PRF/5 cells (Fig. 4*C*). The cytolytic activity against epirubicin-treated HCC cells was significantly decreased to the control levels by adding the anti-MICA/B blocking antibody. These results showed that the addition of epirubicin enhanced the NK sensitivity of HCC cell through increased

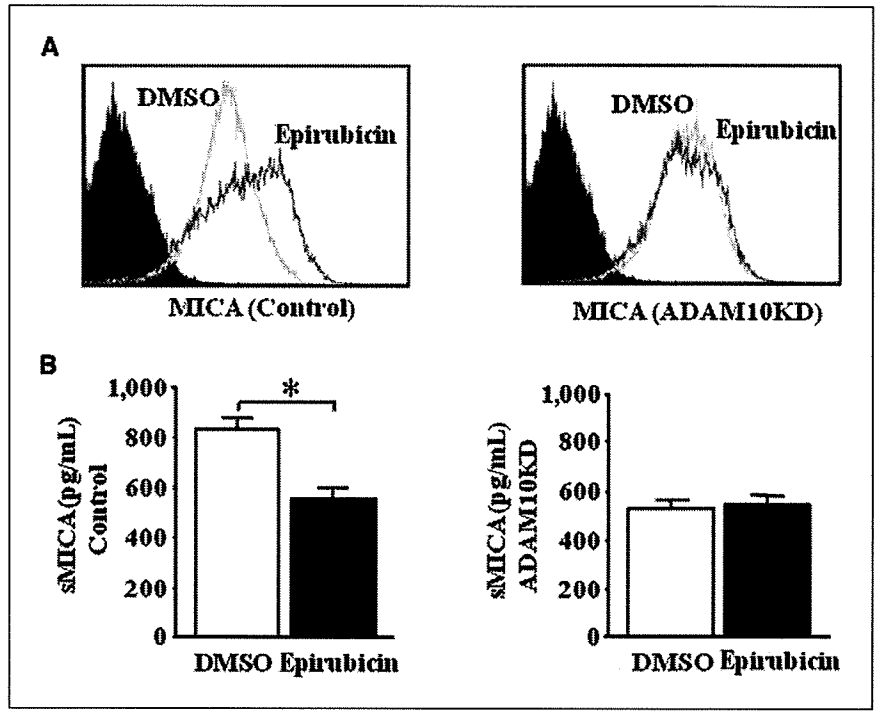

Figure 5. The epirubicin-mediated modification of MICA is ADAM10 dependent. HepG2 cells were transfected with ADAM10 siRNA (*ADAM10KD*) or control siRNA (*Control*) and further cultured with 1 μg/mL of epirubicin (*black lines*) or vehicle (DMSO, *gray line*) for 24 h. The expression of membrane-bound MICA (*MICA*) was evaluated by flow cytometry (*A*), and the soluble MICA (*sMICA*) production in the culture supernatant was evaluated by specific ELISA (*B*). Similar results were obtained from two independent experiments. *, $P < 0.05$.

expression of membrane-bound MICA, although the possibility of MICB involvement could not be excluded. The doxorubicin-treated human HCC cells showed similar results to those obtained from epirubicin-treated HCC cells (data not shown).

Epirubicin inhibits MICA ectodomain shedding through suppression of ADAM10. To examine whether the suppressive effect of epirubicin on MICA shedding occurred through downregulation of ADAM10, HepG2 cells were transfected with ADAM10 siRNA or scramble siRNA as a control and then treated with epirubicin. Consistent with earlier observations, epirubicin upregulated MICA surface expression and downregulated the levels of soluble MICA in control cells (Fig. 5). In contrast, neither upregulation of surface MICA nor downregulation of soluble MICA levels was observed in ADAM10KD-HepG2 cells. These results suggest that the suppressive effect of epirubicin on MICA shedding is mediated by ADAM10 downregulation. We also found similar results with ADAM10KD-PLC/PRF/5 cells (data not shown).

Soluble CD44 and soluble MICA levels in patients with HCC. We have shown that ADAM10 is expressed in human HCC tissues. However, it is not clear whether ADAM10 activity in HCC tissues is actually involved in MICA shedding in patients. Because ADAM10 was reported to be the constitutive functional sheddase of CD44 (23), we examined the soluble CD44 levels in HCC patients, which might be produced from tumor cells through ADAM10 activity. As shown in Fig. 6*A*, the soluble CD44 levels in HCC patients (n = 97) were significantly higher than those in age-matched healthy volunteers (n = 32). More importantly, soluble MICA levels in HCC patients significantly correlated with soluble CD44 levels (Fig. 6*B*), suggesting a close link between MICA shedding and ADAM10 activity.

We further examined soluble CD44 levels before and 2 weeks after TACE in HCC patients. Whereas the levels did not change in nontreated HCC patients during the 2-week interval (n = 9; 306.7 ± 82.5 ng/mL and 309.9 ± 79.9 ng/mL after 2 weeks), they were significantly decreased in epirubicin-based TACE-treated HCC patients (n = 21; 339.7 ± 78.1 ng/mL before TACE and 308.9 ± 81.4 ng/mL after TACE, $P < 0.003$). The changes of soluble CD44 in TACE treatment correlated significantly with those of soluble MICA (P = 0.0002; Fig. 6*C*). These results indicated that ADAM10-mediated CD44 shedding was decreased after TACE in HCC patients, implying that this reduction of ADAM10 activity might be related to the decline in MICA shedding.

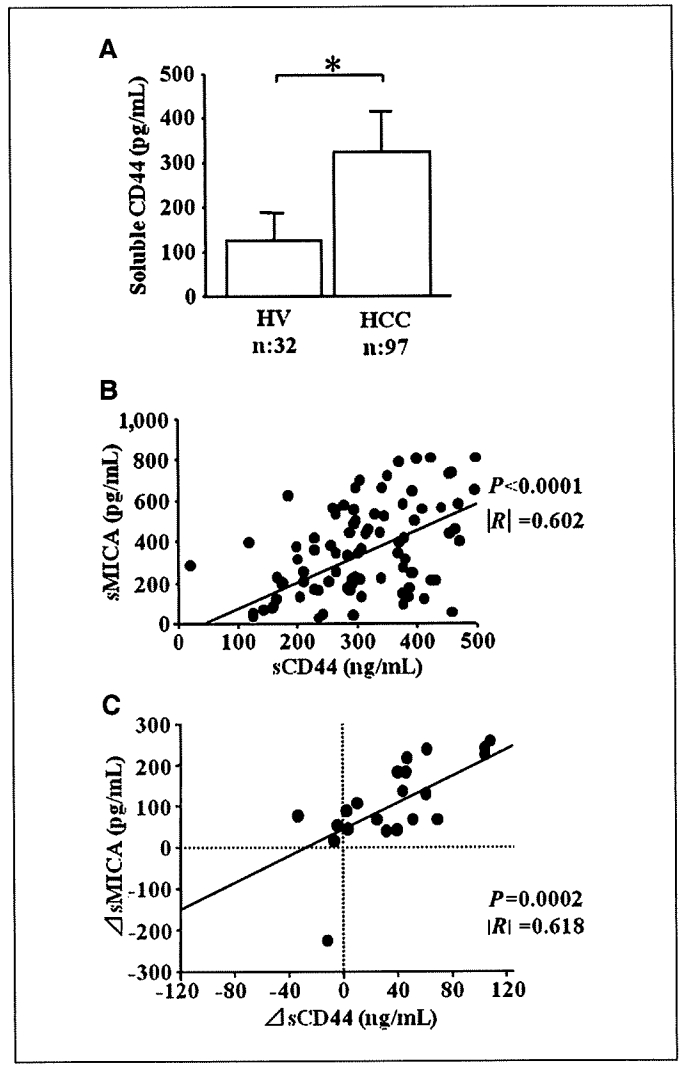

Figure 6. Correlation between soluble CD44 and soluble MICA in human HCC patients. *A* and *B*, soluble CD44 levels and MICA levels in healthy volunteers and HCC patients. Soluble CD44 levels (*sCD44*) and soluble MICA levels (*sMICA*) were determined for sera of HCC patients (n = 97) and age-matched healthy volunteers (*HV*; n = 32). *A*, comparison of sCD44 levels between groups; *B*, correlation between sCD44 levels and sMICA levels in 97 HCC patients. *, $P < 0.05$. *C*, correlation of sCD44 levels and sMICA levels during TACE therapy. HCC patients (n = 21) treated with epirubicin-based TACE therapy were enrolled and examined for sMICA and sCD44 levels before and 2 wk after therapy. Changes in sMICA (ΔsMICA = serum level of sMICA before TACE treatment − serum level of sMICA after TACE treatment) and those in sCD44 levels (ΔsCD44 = serum level of sCD44 before TACE treatment − serum level of sCD44 after TACE treatment) are plotted.

Discussion

MICA shedding is thought to be a principal mechanism by which tumor cells escape from NKG2D-mediated immunosurveillance (13). Thus, inhibition of MICA shedding should be a reasonable strategy for enhancing antitumor immunity. In the present study, we showed that ADAM10 was overexpressed in human HCC tissues and that ADAM10 knockdown resulted in increased expression of membrane-bound MICA, decreased production of soluble MICA, and upregulation of NK sensitivity of human HCC cells. These results point to ADAM10 as a therapeutic target for inhibiting MICA shedding, thereby ameliorating immunity against HCC. Waldhauer and colleagues recently showed that both ADAM10 and ADAM17 proteases are critically involved in the proteolytic release of soluble MICA of human 293T fibroblast cells and HeLa cervix carcinoma cells (20). Interestingly, in the present study, ADAM17 knockdown failed to affect MICA expression in human HepG2 cells or PLC/PRF/5 cells. Thus, ADAM10, not ADAM17, plays an essential role in the shedding of MICA in human HCC cells. Anderegg and colleagues (23) reported that only ADAM10, not ADAM17, contributed to shedding of CD44 molecules in human melanoma cells although both ADAM10 and ADAM17 proteases were significantly expressed in human melanoma tissues, suggesting that ADAM10 and ADAM17 do not always work in a similar manner. A recent report showed that ADAM10, but not ADAM17, could directly bind to calmodulin (24), which may involve the difference of MICA cleavage between ADAM10 and ADAM17 proteases. Recently, Boutet and colleagues reported that ADAM17 regulates proteolytic shedding of the MICB protein, which is another ligand for the NKG2D receptor on immune cells (25). We previously showed that both soluble MICA and MICB significantly increased in the sera of HCC patients and that therapeutic intervention for HCC leads to reduction of soluble

MICA levels, but not of soluble MICB levels (17), suggesting a more important role of soluble MICA in regulating NKG2D expression after HCC therapy. This led us to focus on the mechanism of MICA shedding in the present study.

Our results revealed that anticancer drugs such as epirubicin and doxorubicin downregulated ADAM10 expression and activity, thereby inhibiting MICA ectodomain shedding. The ADAM family proteins, which are highly expressed in some tumors, play a role in secreting growth factors, such as HB-EGF, and migration of cells. Thus, it is speculated that these proteins could be potential targets for tumor treatment (22). The present study is the first to show that clinically available anticancer drugs have an ability to modulate the expression of ADAM family proteins. They seem to suppress ADAM10 expression at a transcriptional level, but the precise mechanism of this suppression is not yet known.

The MICA ELISA system may not equally detect all soluble MICA (MICA molecules have >60 allelic variants). Our finding that soluble MICA could be detected in all HCC patients suggests that this system was applicable for our cohort of HCC patients. However, special caution should be paid for the use of this ELISA system for widely polymorphic MICA. Because CD44 is well known to be released into circulation from tumors by proteolytic cleavage of ADAM10 (23), the activity of ADAM10 in HCC tissues may be correlated with soluble CD44 levels. If so, our data suggest a close link between ADAM10 activity and the shedding of MICA in HCC. Furthermore, the decline in soluble MICA levels correlated well with the decline in soluble CD44 levels as early as 2 weeks after epirubicin-based TACE therapy. Reducing the tumor volume by such therapy may have led to both decreases but it is also possible that epirubicin suppresses ADAM10 activity, thereby inhibiting the shedding of MICA and CD44. Epirubicin may have a previously unrecognized role in cancer therapy; that is, affecting ADAM10 activity and MICA shedding rather than simply serving as a direct toxic agent for tumor cells.

Our data suggest that anti-HCC chemotherapy could remodel HCC cells, enhancing sensitivity to NK cells by upregulating MICA expression on the cellular surface. A concomitant decline in soluble MICA levels ameliorates NK cell ability by upregulating its NKG2D expression. We previously showed that activation of local innate antitumor immunity in liver tissues resulted in eliciting tumor-specific acquired immunity (21). If liver innate immunity is efficiently activated after anti-HCC chemotherapy, an additional antitumor effect against HCC cells could be expected. Immune modulators such as α-galactosylceramide have been shown to efficiently activate liver innate immune cells, including NK cells (21, 26). The combination therapy of anti-HCC chemotherapy and immunotherapy targeting NK cells might improve the antitumor effect of unresectable HCC and the prognosis of HCC patients.

In spite of recent progress in HCC therapies, there remains significant room for improvement, especially with respect to advanced liver cancer. We have shown here that anti-HCC chemotherapy resulted in enhanced NK sensitivity of HCC cells through inhibition of the activity of ADAM10 protease followed by modification of MICA expression. These findings indicate that efficient activation of liver innate immunity after anti-HCC chemotherapy might represent a particularly promising approach to suppress tumor growth and promote regression in liver cancer patients.

Disclosure of Potential Conflicts of Interest

No potential conflicts of interest were disclosed.

Acknowledgments

Received 3/4/09; revised 7/15/09; accepted 7/24/09; published OnlineFirst 10/13/09.

Grant support: Grant-in-Aid from the Ministry of Education, Culture, Sports, Science and Technology of Japan (T. Takehara) and Grant-in-Aid for Research on Hepatitis and BSE from the Ministry of Health, Labour and Welfare of Japan (N. Hayashi).

The costs of publication of this article were defrayed in part by the payment of page charges. This article must therefore be hereby marked *advertisement* in accordance with 18 U.S.C. Section 1734 solely to indicate this fact.

References

1. Fattovich G, Stroffolini T, Zagni I, Donato F. Hepatocellular carcinoma in cirrhosis: incidence and trends. Gastroenterology 2004;127:S35–50.
2. Bosch FX, Ribes J, Diaz M, Cleries R. Primary liver cancer: worldwide incidence and trends. Gastroenterology 2004;127:S5–16.
3. Takayasu K, Arii S, Ikai I, et al. Prospective cohort study of transarterial chemoembolization for unresectable hepatocellular carcinoma in 8510 patients. Gastroenterol 2006;131:461–9.
4. Doherty DG, O'Farrelly C. Innate and adaptive lymphoid cells in human liver. Immunol Rev 2000;174:5–20.
5. Mehal WZ, Azzaroli F, Crispe IN. Immunology of the healthy liver: old questions and new insights. Gatsroenterology 2001;120:250–60.
6. Bauer S, Groh V, Wu J, et al. Activation of NK cells and T cells by NKG2D, a receptor for stress-inducible MICA. Science 1999;285:727–9.
7. Groh V, Rhinehart R, Seceist H, Bauer S, Grabstein KH, Spies T. Broad tumor-associated expression and recognition by tumor-derived γδT cells of MICA and MICB. Proc Natl Acad Sci U S A 1999;96:6879–84.
8. Jinushi M, Takehara T, Tatsumi T, et al. Expression of MICA and MICB in human hepatocellular carcinomas and their regulation by retinoic acids. Int J Cancer 2003;104:354–61.
9. Wu JD, Higgins LM, Steinle A, Cosman D, Haugk K, Plymate SR. Prevalent expression of the immunostimulatory MHC class I chain-related molecule is counteracted by shedding in prostate cancer. J Clin Invest 2004;114:560–8.
10. Raffaghello L, Prigione I, Airoldi I, et al. Downregulation and/or release of NKG2D ligands as an immune evasion strategy of human neuroblastoma. Neoplasia 2004;6:558–68.
11. Ogasawara K, Lanier LL. NKG2D in NK and T cell-mediated immunity. J Clin Immunol 2005;25:534–40.
12. Coudert JD, Held W. The role of the NKG2D receptor for tumor immunity. Semin Cancer Biol 2006;16:333–43.
13. Groh V, Wu J, Yee C, Spies T. Tumor-derived soluble MIC ligands impair expression of NKG2D and T cell activation. Nature 2002;419:734–8.
14. Salih HR, Rammensee HG, Steinle A. Downregulation of MICA on human tumors by proteolytic shedding. J Immunol 2002;169:4098–102.
15. Salih HR, Antropius H, Gieseke F, et al. Functional expression and release of ligands for activating immunoreceptor NKG2D in leukemia. Blood 2003;102:1389–96.
16. Jinushi M, Takehara T, Tatsumi T, et al. Impairment of natural killer cell and dendritic cell functions by soluble form of MHC class I-related chain A in advanced human hepatocellular carcinoma. J Hepatol 2005;43:1013–20.
17. Kohga K, Takehara T, Tatsumi T, et al. Serum levels of soluble major histocompatibility complex (MHC) class I-related chain A in patients with chronic liver disease and changes during transcatheter arterial embolization for hepatocellular carcinoma. Cancer Sci 2008;99:1643–9.
18. Holdenrieder S, Stieber P, Peterfi A, Nagel D, Steinle A, Salih HR. Soluble MICA in malignant disease. Int J Cancer 2006;118:684–7.
19. Kaiser BK, Yim D, Chow IT, et al. Disulphide-isomerase-enabled shedding of tumor-associated NKG2D ligands. Nature 2007;447:482–6.
20. Waldhauer I, Goehlsdorf D, Gieseke F, et al. Tumor-associated MICA is shed by ADAM proteases. Cancer Res 2008;68:6368–76.
21. Tatsumi T, Takehara T, Yamaguchi S, et al. Intrahepatic delivery of α-galactosylceramide-pulsed dendritic cells suppresses liver tumor. Hepatology 2007;45:22–30.
22. Mochizuki S, Okada Y. ADAMs in cancer cell proliferation and progression. Cancer Sci 2007;98:161–7.
23. Anderegg U, Eichenberg T, Parthaune T, et al. Simon JC. ADAM10 is the constitutive functional sheddase of CD44 in human melanoma cells. J Invest Dermatol 2009;129:1471–82.
24. Nagano O, Murakami D, Hartmann D, et al. Cell-matrix interaction via CD44 is independently regulated by different metalloproteinases activated in response to extracellular domain Ca^{2+} influx and PKC activation. J Cell Biol 2004;165:893–902.
25. Boutet P, Aguera-Gonzalez S, Atkinson S, et al. The metalloproteinase ADAM17/TNF-α enzyme regulates proteolytic shedding of the MHC class I-related chain B protein. J Immunol 2009;182:49–53.
26. Miyagi T, Takehara T, Tatsumi T, et al. CD1d-mediated stimulation of natural killer T cells selectively activates hepatic natural killer cells to eliminate experimentally disseminated hepatoma cells in murine liver. Int J Cancer 2003;106:81–9.

Cancer Immunol Immunother (2010) 59:453–463
DOI 10.1007/s00262-009-0764-x

ORIGINAL ARTICLE

Natural killer cell is a major producer of interferon γ that is critical for the IL-12-induced anti-tumor effect in mice

Akio Uemura · Tetsuo Takehara · Takuya Miyagi · Takahiro Suzuki · Tomohide Tatsumi · Kazuyoshi Ohkawa · Tatsuya Kanto · Naoki Hiramatsu · Norio Hayashi

Received: 12 February 2009 / Accepted: 24 August 2009 / Published online: 16 September 2009

Abstract Although the anti-tumor effect of IL-12 is mediated mostly by IFNγ, which cell types most efficiently produce IFNγ and therefore initiate or promote the anti-tumor effect of IL-12 has not been clearly determined. In the present study, we demonstrated hydrodynamic injection of the IL-12 gene led to prolonged IFNγ production, NK-cell activation and complete inhibition of liver metastasis of CT-26 colon cancer cells in wild-type mice, but not in IFNγ knockout mice. NK cells expressed higher levels of STAT4 and upon IL-12 administration displayed stronger STAT4 phosphorylation and IFNγ production than non-NK cells. Adoptive transfer of wild-type NK cells into IFNγ knockout mice restored IL-12-induced IFNγ production, NK-cell activation and anti-tumor effect, whereas transfer of the same number of wild-type non-NK cells did not. In conclusion, NK cells are predominant producers of IFNγ that is critical for IL-12 anti-tumor therapy.

Keywords IFNγ · Innate immunity · Liver tumor · IL-12 · NK

A. Uemura and T. Takehara contributed equally to this work.

Electronic supplementary material The online version of this article (doi:10.1007/s00262-009-0764-x) contains supplementary material, which is available to authorized users.

A. Uemura · T. Takehara · T. Miyagi · T. Suzuki · T. Tatsumi · K. Ohkawa · T. Kanto · N. Hiramatsu · N. Hayashi (✉)
Department of Gastroenterology and Hepatology,
Osaka University Graduate School of Medicine,
2-2 Yamada-oka, Suita, Osaka 565-0871, Japan
e-mail: hayashin@gh.med.osaka-u.ac.jp

A. Uemura
e-mail: akioue@gh.med.osaka-u.ac.jp

Introduction

IL-12 is a 70-kDa heterodimer protein, composed of p35 and p40 subunits, mainly produced by antigen-presenting cells. IL-12 was originally found as a "natural killer-stimulating factor" and a "cytotoxic lymphocyte maturation factor" [1, 2]. IL-12 has multi-potent effects, inducing a Th1 response, enhancing the CD8 T-cell response, activating natural killer cells and inducing production of IFNγ [3, 4]. Therapeutic use of IL-12, either using its recombinant protein or gene, can induce an efficient anti-tumor effect on primary or metastatic tumors in various murine models and humans [5, 6].

Research has shown that IL-12 mediates anti-tumor effects in a variety of ways. They include anti-proliferative effects, anti-angiogenic effects [7, 8] and cytotoxic effects of effector lymphocytes. A variety of effector cells has been reported to be required for IL-12-mediated anti-tumor effects: they include CD8 T cells [9], NKT cells [10], CD4 T cells [11] and NK cells [12]. The relative contribution of these cells may differ among IL-12 doses and types of tumor models [13]. Endogenous IFNγ production is required for most, if not all, of the anti-tumor effects of IL-12 administration [14, 15]. IL-12 stimulates a variety of immune cells, such as T cells [16], B cells [17] and NK cells [18], to produce IFNγ. However, which cell types are most critical for producing IFNγ during IL-12 therapy is not clearly known.

In the present study, we used a murine model of liver metastasis of CT-26 colon cancer cells and found that NK cells highly expressed the IL-12 signaling molecule STAT4 and most efficiently produced IFNγ. IFNγ was essential for the anti-tumor effect of IL-12, and NK-cell production of IFNγ sufficed to produce the full-blown anti-tumor effects. These results demonstrated that NK cells

serve not only as an effector but also as an important mediator producing IFNγ that is critical for the anti-tumor effects of IL-12.

Materials and methods

Mice

Specific pathogen-free female Balb/c mice were purchased from Clea Japan, Inc (Tokyo, Japan). Rag2 knockout (Rag2 KO) mice with a Balb/c background were purchased from Taconic (Germantown, NY). IFNγ knockout (GKO) mice with a Balb/c background were kindly provided by Dr. Yoichiro Iwakura (Institute of Medical Science, University of Tokyo). All mice used were at the age of 6 to 10 weeks. They were housed under conditions of controlled temperature and light with free access to food and water at the Institute of Experimental Animal Science, Osaka University Graduate School of Medicine. All animals received humane care, and the study protocol complied with the institution's guidelines.

Tumor models

Intra-splenic injection of tumor cells was used to establish micro-disseminated liver tumors in mice [19]. CT-26 colon cancer cells originating from Balb/c mice were maintained in RPMI1620 supplemented with 10% FCS. Syngeneic mice were anesthetized with pentobarbital and given a cut on the left side flank. CT-26 cells (1×10^5) were suspended in 200 μl of PBS and injected into the spleen.

Injection of naked plasmid DNA

A plasmid coding the murine IL-12 gene, pCMV-IL-12, was generously provided by Dr. M Watanabe (Laboratory of Experimental Immunology, Division of Basic Sciences, National Cancer Institute-Frederick Cancer Research and Development Center) [20]. Plasmid DNA was prepared using an EndoFree plasmid system (Qiagen, Hilden, Germany,) according to the manufacturer's instructions. Hydrodynamic injection of plasmid DNA was performed as previously described [21]. In brief, 25 μg of plasmid DNA was diluted with 2.0 ml of lactated Ringer's solution and injected into the tail vein, using a syringe with a 26-gauge needle. DNA injection was completed within 5 to 8 s.

ELISA

Blood samples were serially obtained from the venous plexus in the retro-orbita under light anesthesia. The levels of serum IL-12 p70, IFNγ (BD Biosciences-Pharmingen, San Diego, CA), IFNγ-inducible protein 10 (IP-10) and monokine induced by IFNγ (MIG) (R&D Systems, Inc, Minneapolis, MN) were measured using commercially available ELISA kits in accordance with the manufacturer's instructions.

Mononuclear cells

Mononuclear cells were isolated from the liver or spleen as previously described. The NK activity of mononuclear cells was assessed by a standard 4-h ^{51}Cr-releasing assay using Yac1 cells as targets. In some experiments, mononuclear cells were separated into $DX5^+$ cells (NK cells) and $DX5^-$ cells (non-NK cells) using the MACS system (Miltenyi Biotec GmbH, Bergisch Gladbach, Germany). The purity of the isolated NK-cell population was found to be greater than 90% by FACS analysis.

Flow cytometric analysis

Liver mononuclear cells were isolated 2 days after pCMV-IL-12 injection. Cytokine secretion was then blocked by the addition of brefeldin A for 4 h. Next, liver mononuclear cells were stained with FITC-conjugated anti-TCRβ antibody and biotin-conjugated anti-CD49b antibody (DX5), fixed and permeabilized with Cytofix/Cytoperm (BD Biosciences), and stained with PE-conjugated anti-INFγ antibody or corresponding isotype controls. Analysis was performed using a FACSCalibur (Becton Dickinson), with the resulting data analyzed using the CELLQuest program (Becton Dickinson). NK cells were identified as $DX5^+/TCR\beta^-$ lymphocytes, NKT cells as $DX5^+/TCR\beta^+$ lymphocytes and T cells as $DX5^-/TCR\beta^+$ lymphocytes.

Adoptive transfer

For adoptive transfer experiments, GKO mice were injected intravenously 1 day before plasmid DNA injection with 2.0×10^8 whole mononuclear cells or 4.0×10^6 NK cells, or non-NK cells or whole mononuclear cells, all of which had been harvested from wild-type mice that can produce IFNγ.

Western blotting

Mouse recombinant IL-12 was purchased from R&D Systems, Inc (Minneapolis, MN). Mononuclear cells were treated with or without IL-12. Whole cell lysate was prepared from mononuclear cells from mice, and 20 μg of protein was separated by SDS-PAGE and transferred to the PVDF membrane. The membrane was stained with anti-STAT4 antibody (BD biosciences),

anti-phospho-specific STAT4 (pY693) antibody (BD biosciences), anti-STAT1 antibody (Cell Signaling), anti-phospho-specific STAT1 antibody (Cell Signaling) and visualized by chemiluminescence.

NK-cell depletion

For depletion of NK cells in vivo, anti-asialoGM1 antibody (WAKO, Osaka, Japan) was intraperitoneally administered. We determined the appropriate dosing to be 500 μg/mouse (50 μl when dissolved according to the manufacturer's instructions) based on FACS analysis of hepatic mononuclear cells. The percentage of $DX5^+/TCR\beta^-$ cells (NK cells) is 12.6 ± 2.4% in IgG-injected liver, whereas it decreased to 0.76 ± 0.04% one day after anti-asialo GM1 antibody injection ($N = 3$/group). This effect remained at least 3 days after anti-asialo GM1 antibody injection. NKT cells were less affected than NK cells, because 90% of $DX5^+/TCR\beta^+$ cells (NKT cells) still remained in the liver after the treatment. Anti-asialoGM1 antibody was injected 1 day after tumor inoculation and then every 5 days. For the control, the same amount of normal rabbit immunoglobulin (DAKO, Copenhagen, Denmark) was intraperitoneally administered.

Histology

The formalin-fixed livers were paraffin-embedded, and liver sections were analyzed by hematoxylin-eosin staining. Acetone-fixed fresh frozen liver sections were immunostained with anti-mouse CD4 (H123.19), anti-mouse CD8α (53-6.7) or anti-CD31 (390) monoclonal antibody (all from BD Biosciences), using a VECSTAIN ABC kit (Vector Laboratories, Burlingame, California, USA).

Statistics

Data are represented as mean ± SD. Comparisons between groups were analyzed by unpaired t-test with Welch's correction. $p < 0.05$ was considered statistically significant.

Results

Hydrodynamic injection of IL-12-expressing plasmid led to prolonged production of IFNγ

Hydrodynamics-based gene delivery into mice establishes efficient foreign gene expression predominantly in the liver, especially in hepatocytes. Serial measurement of serum IL-12 demonstrated that pCMV-IL-12 injection led to substantial IL-12 production on day 1. The levels of serum IL-12 then rapidly declined (Fig. 1a). We also measured IFNγ production in serum, since IL-12 is known to activate IFNγ production. pCMV-IL-12 and, to a lesser extent, pCMV injection increased serum IFNγ on day 1. In contrast to the pCMV injection group, high levels of serum IFNγ were maintained at later time points in the pCMV-IL-12 injection group (Fig. 1a). Thus, hydrodynamic injection of pCMV-IL-12 led to prolonged production of IFNγ. Transient IFNγ production followed by control plasmid may be an indirect effect of liver injury caused by bolus injection of saline or DNA injection.

IL-12 therapy induced NK activation and anti-metastatic effects, both of which are critically dependent on IFNγ

To examine the biological effects of the produced IL-12, we evaluated the NK activity of mononuclear cells from the liver. pCMV-IL-12 injection, but not control pCMV injection, increased Yac1 lytic activity of hepatic mononuclear cells (Fig. 1b). When GKO mice were injected with pCMV-IL-12 or pCMV, the hepatic mononuclear cells did not display any lytic ability to Yac1 cells, suggesting that IL-12-mediated NK-cell activation required IFNγ.

To examine the anti-metastatic effect of IL-12, pCMV-IL-12 or pCMV was injected into wild-type mice 2 days after intrasplenic injection of CT-26 cells. At 14 days after tumor injection, the mice were killed for evaluation of liver tumor (Fig. 1c). While pCMV-injected mice displayed huge liver tumors, pCMV-IL-12-injected mice did not show any macroscopic or microscopic tumor (Fig. 1d). Liver weight was significantly higher in pCMV-injected mice than pCMV-IL-12-injected mice, reflecting liver tumor formation. To examine the involvement of IFNγ in the IL-12-induced anti-tumor effect, we injected pCMV or pCMV-IL-12 into GKO mice 2 days after CT-26 injection. At 14 days after CT-26 injection, both groups showed similar degrees of tumor formation and there was no significant difference in liver weight between the two. This indicated that IL-12-induced anti-metastatic effect was strictly dependent on IFNγ.

NK cells were the most potent producer of IFNγ during IL-12 therapy

To evaluate which cell types most efficiently produced IFNγ, we isolated hepatic mononuclear cells from mice 2 days after plasmid injection and then stained cell surface TCRβ and DX5 as well as intracellular IFNγ (Fig. 2). $TCR\beta^-/DX5^+$ NK cells, $TCR\beta^+/DX5^+$ NKT cells and $TCR\beta^+/DX5^-$ T cells from pCMV-IL-12-injected mice showed significant levels of IFNγ production compared

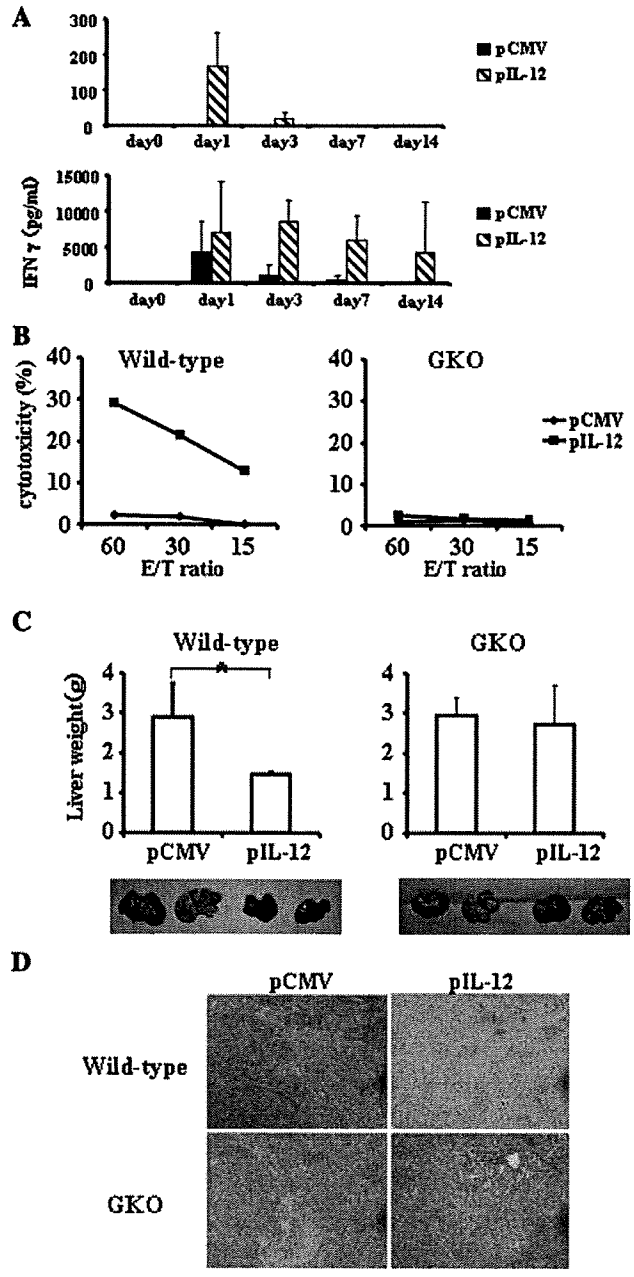

Fig. 1 Effects of hydrodynamic injection of IL-12-encoding plasmid. **a** Wild-type mice were hydrodynamically injected with either pCMV-IL-12 (*hatched bars*) or pCMV (*closed bars*) and bled at the indicated time points to measure the levels of serum IL-12 and IFNγ. Results are indicated as mean and SD ($n = 6$/group). **b** NK-cell activation after IL-12 administration. Hepatic mononuclear cells were isolated from wild-type mice (*left*) or GKO mice (*right*) which had been injected with pCMV-IL-12 (*closed squares*) or pCMV (*closed diamonds*) 4 days earlier. Yac1 lytic ability was measured by a standard ^{51}Cr-release assay at the indicated effector and target ratios (E/T ratio). All experiments were performed at least 3 times and representative data are shown. **c** and **d** Anti-metastatic effects of IL-12 therapy. Wild-type mice (*left*) or GKO mice (*right*) were intrasplenically injected with CT-26 cells and, 2 days later, hydrodynamically injected with either pCMV-IL-12 or pCMV. At 14 days after the plasmid injection, the mice were killed to examine liver tumor development. **c** Data are indicated as mean and SD of the liver weight at the top ($n = 6$/group) and a representative picture of the liver in each group is shown at the bottom. *$p < 0.001$. **d** Representative histology of liver sections

with those from naive mice or pCMV-injected mice. The levels of IFNγ production were highest in NK cells among those cells. Even at a later time point, 7 days after plasmid injection, NK cells were found to produce the highest levels of IFNγ (data not shown).

IL-12-induced STAT4 signaling and IFNγ production increased in NK cells

IL-12 activates Janus kinases Tyk2 and Jak2, STAT4 as well as other STATs. To examine the activation of STAT1 and STAT4, we isolated splenocytes from wild-type mice and GKO mice and stimulated them with IL-12 and/or IFNγ in the presence or absence of anti-IFNγ Ab (Fig. 3a). IL-12 led to phosphorylation of both STAT1 and STAT4 in wild-type splenocytes. In contrast, the same treatment led to phosphorylation of STAT4, but not of STAT1, in GKO splenocytes. Addition of IFNγ restored STAT1 phosphorylation in GKO splenocytes. Furthermore, adding anti-IFNγ inhibited STAT1 phosphorylation in wild-type cells. These findings demonstrated that phosphorylation of STAT4 is a direct effect of IL-12 but phosphorylation of STAT1 is indirect, via an autocrine or paracrine IFNγ-dependent manner.

To examine STAT1 and STAT4 activation and IFNγ production in NK cells and non-NK cells, we prepared whole mononuclear cells as well as NK and non-NK populations from wild-type spleens and stimulated the cells with IL-12 (Fig. 3b). NK cells expressed higher levels of STAT4 than non-NK cells. Upon IL-12 treatment, STAT4 was rapidly phosphorylated in NK cells, but to a lesser extent in non-NK cells. In contrast, NK cells expressed lesser levels of STAT1 than non-NK cells. STAT1 was similarly phosphorylated in NK cells and non-NK cells upon IL-12 treatment. Both NK cells and non-NK cells produced significant levels of IFNγ, but the levels were much higher in NK cells than non-NK cells (Fig. 3c). These results indicated that compared with non-NK cells, NK cells possessed higher levels of STAT4, a direct signaling molecule of IL-12, and produced higher levels of IFNγ than non-NK cells.

NK cells were sufficient for IL-12-mediated anti-tumor effects

The above observation indicated that NK cells are a predominant producer of IFNγ, which was critical for the IL-12-induced anti-tumor effects. To examine whether NK

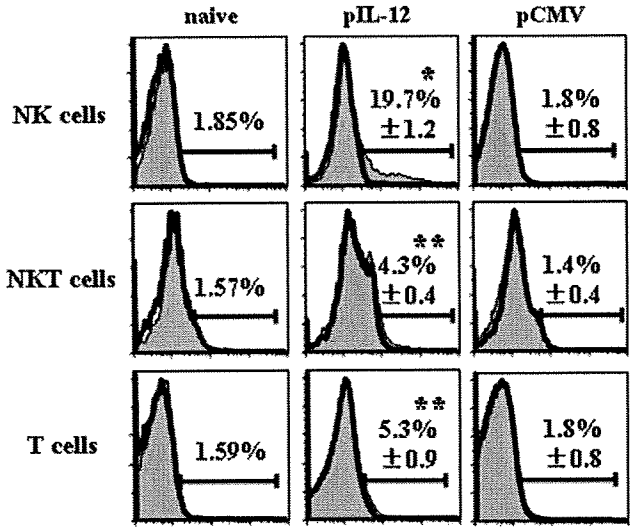

Fig. 2 IFNγ expression of mononuclear cells after IL-12 administration. Wild-type mice were injected with pCMV-IL-12 or pCMV, or were untreated (naive). Mononuclear cells were isolated from the liver 2 days after plasmid injection and stained with anti-TCRβ mAb, anti-DX5 mAb and anti-IFNγ mAb. *Closed histograms* show the IFNγ expression in the gated populations ($TCR\beta^+/DX5^+$ cells for NK cells, $TCR\beta^+/DX5^+$ cells for NKT cells and $TCR\beta^+/DX5^-$ cells for T cells). Isotype control stainings are shown by *open histograms*. Numbers in histograms represent averages ± SD of percentages of positive cells ($n = 3$ mice/group). $*p < 0.0001$ vs. mock in NK populations. $**p < 0.05$ vs. mock in each population

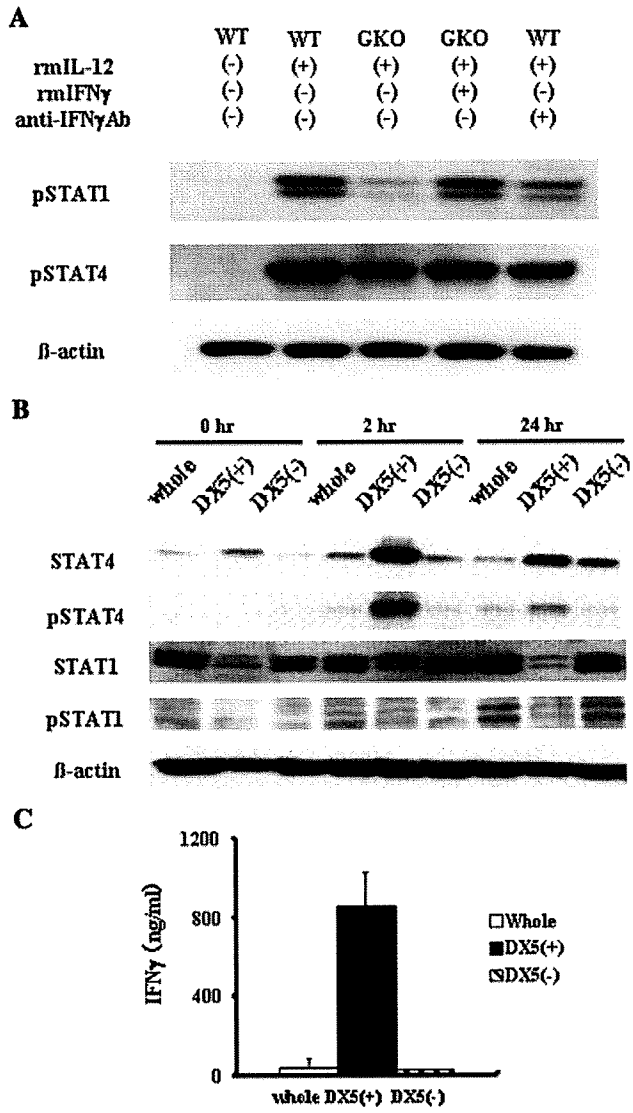

Fig. 3 STAT signaling and IFNγ production of mononuclear cells in vitro treated with IL-12. **a** STAT1 and STAT4 activation of splenocytes in vitro treated with IL-12. Splenocytes were isolated from wild-type mice or GKO mice and treated with or without recombinant IL-12 (20 ng/mL) in the presence or absence of recombinant IFNγ (500 ng/mL) or anti- IFNγ antibody (20 μg/mL) for 24 h. Cellular lysates were analyzed by Western blot for the expression of phospho-STAT1, phospho-STAT4 and β-actin. **b** and **c** STATs expression and signaling of NK cells and non-NK cells. Splenocytes were isolated from wild-type mice. Whole splenocytes were further purified into $DX5^+$ cells and $DX5^-$ cells. Each cell population was cultured with recombinant IL-12 (20 ng/mL) for the indicated times. **b** The cells were lysed to examine expression of whole STAT and phospho-STAT by Western blot. **c** The levels of IFNγ in the culture supernatant at 24 h were determined by ELISA. Data are expressed as mean and SD ($n = 3$)

cells are sufficient for the anti-metastatic effects of IL-12, we examined the anti-metastatic effect in Rag2 KO mice which lack T cells, B cells and NKT cells. pCMV-IL-12 injection enhanced the Yac1 lytic ability of hepatic mononuclear cells in Rag2 KO mice higher than in wild-type mice (Fig. 4a). To examine whether NK cells are sufficient for IL-12-mediated rejection of hepatic metastasis, we injected pCMV-IL-12 or pCMV into mice that had been intra-splenically injected with CT-26 cells 2 days earlier. Serum IFNγ levels of Rag2 KO mice were about 4 times higher than those of wild-type mice (Fig. 4b). pCMV-IL-12 completely suppressed hepatic metastasis in Rag2 KO mice (Fig. 4c).

Adoptive transfer of wild-type NK cells into GKO mice restored the anti-tumor effects of IL-12

Since NK cells were sufficient for producing IL-12-induced anti-tumor effects, we postulated that their production of IFNγ may play an important role in these effects. To test this, we performed adoptive transfer experiments with GKO mice. First, whole mononuclear cells isolated from the spleens of wild-type mice (2.0×10^8 cells) were adoptively transferred to GKO mice 1 day before plasmid injection. pCMV-IL-12 injection increased Yac1 lytic activity of hepatic mononuclear cells in the adoptively transferred group, but not in the untreated group (Fig. 5a). pCMV-IL-12 induced significant increase in serum IFNγ levels 4 days after plasmid injection in the adoptive transferred group, but not in the other groups (Fig. 5b). The

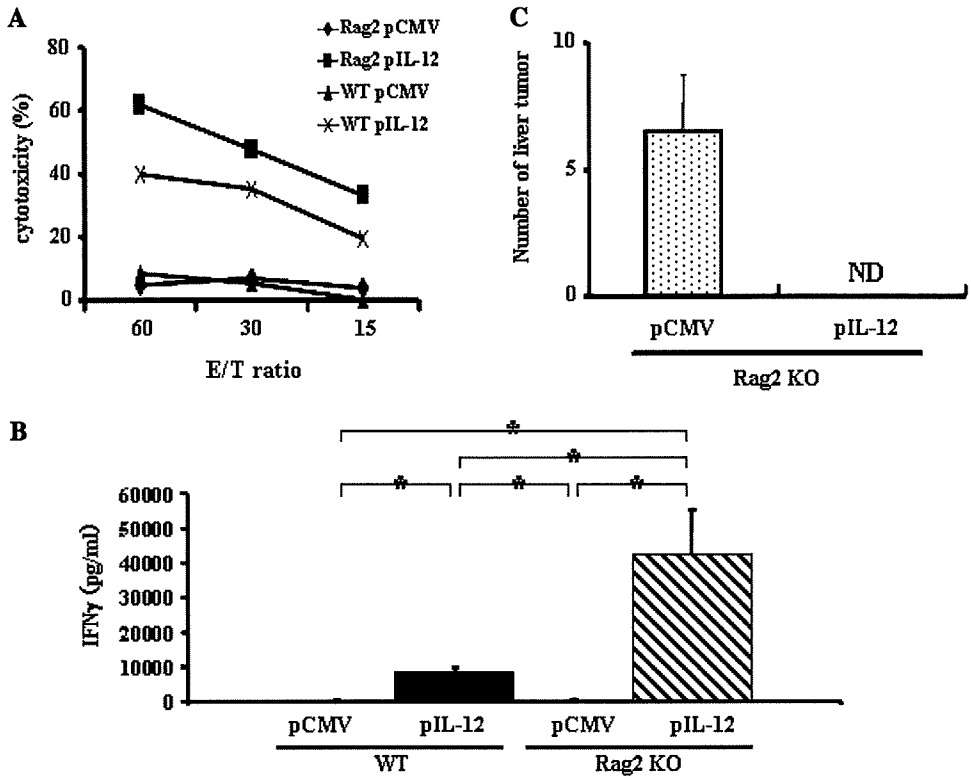

Fig. 4 Anti-tumor effects of IL-12 in Rag2 KO mice. Serum IFNγ levels and NK-cell activation. Wild-type or Rag2 KO mice were hydrodynamically injected with either pCMV-IL-12 or pCMV and killed at 4 days. **a** Yac1 lytic ability of hepatic mononuclear cells was determined by Cr releasing assay as the indicated effector and target ratios (E/T ratio). Experiments were done 2 times and representative data are shown. **b** The levels of serum IFNγ were determined by ELISA. Data are expressed as mean and SD ($n = 7$/group). $^*p < 0.0001$. **c** Anti-metastatic effect. Rag2 KO mice were intrasplenically injected with CT-26 cells and, 2 days later, hydrodynamically injected with either pCMV-IL-12 or pCMV. Fourteen days after plasmid injection, mice were killed to examine tumor development in the liver. The numbers of hepatic tumors in each group are expressed as mean and SD ($n = 7$/group). *ND* not detectable

anti-metastatic effect of IL-12 was restored in GKO mice when whole mononuclear cells from wild-type mice were adoptively transferred (Fig. 5c).

To evaluate the contribution of IFNγ production from each subset of mononuclear cells to the anti-metastatic effect of IL-12, we adoptively transferred the same number of whole mononuclear cells, NK cells or non-NK cells from wild-type mice (4.0×10^6 cells) 1 day before pCMV-IL-12 injection and analyzed liver tumor formation. Only in the NK-cell-transferred group, pCMV-IL-12 injection induced NK cytolytic ability in the liver and IFNγ elevation in serum 4 days after plasmid injection, but not in the other groups (Fig. 5d, e). No liver tumor formed in the NK-cell-transferred group. In contrast, livers in other groups had massive tumors, and the liver weights were significantly heavier than those in the NK-cell-transferred group (Fig. 5f). These results clearly demonstrated the strong impact of IFNγ produced from NK cells on IL-12-induced anti-tumor effects compared with that from non-NK cells.

Anti-tumor effects of IL-12 deteriorated slightly in mice depleted of NK cells

To examine the involvement of NK cells in the tumor deletion by IL-12 therapy, we induced depletion of NK cells by repeatedly injecting anti-asialoGM1 antibody. The cytolytic ability of NK cells was completely abolished in the anti-asialoGM1 antibody-injected group (Fig. 6a). Serum IFNγ induction by IL-12 in the NK depletion group was about half of that in the control immunoglobulin injected group (Fig. 6b). Unexpectedly, pCMV-IL-12 injection inhibited macroscopic liver metastasis of CT-26 cells in NK cell-depleted mice (Fig. 6c). However, a number of microscopic tumor regions were observed after IL-12 therapy in NK cell-depleted mice but not in control IgG-injected mice (Fig. 6d). This finding indicated that NK cells are required for a full-blown IL-12 anti-tumor effect, but IL-12's anti-tumor effect was still observed even if the NK cells were knocked down. To examine the underlying mechanisms of anti-tumor effect in NK cell-depleted mice,

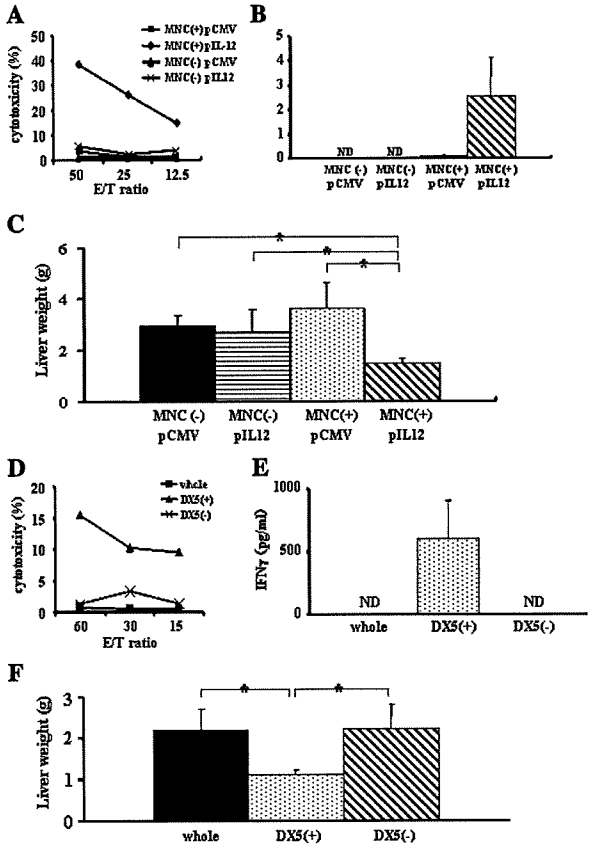

Fig. 5 Adoptive transfer of wild-type cells into GKO mice. Adoptive transfer of wild-type splenocytes restored anti-tumor effects of IL-12 in GKO mice. **a** GKO mice were intravenously injected with or without 2.0×10^8 splenocytes from wild-type mice and, 1 day later, hydrodynamically injected with either pCMV-IL-12 or pCMV. Mice were killed 4 days after plasmid injection. Yac1 lytic ability of hepatic mononuclear cells was expressed as the indicated effector and target ratios (E/T ratio). Experiments were done 3 times and representative data are shown. **b** and **c** GKO mice were intrasplenically injected with CT-26 cells and, 1 day later, intravenously injected with or without 2.0×10^8 splenocytes from wild-type mice. Two days after CT-26 injection, mice were hydrodynamically injected with either pCMV-IL-12 or pCMV. **b** The levels of serum IFNγ 4 days after plasmid injection are expressed as mean and SD (n = 6/group). **c** Fourteen days after plasmid injection, mice were killed to examine liver tumor development by measuring liver weight. The results are indicated as mean and SD (n = 6/group). *ND* not detectable. $^*p < 0.01$. Adoptive transfer of wild-type NK cells, but not non-NK cells, restored anti-tumor effects of IL-12 in GKO mice. **d** Wild-type splenocytes were purified into $DX5^+$ cells and $DX5^-$ cells. GKO mice were intravenously injected with 4.0×10^6 whole mononuclear cells or $DX5^+$ cells or $DX5^-$ cells and, 1 day later, hydrodynamically injected with either pCMV-IL-12 or pCMV. Mice were killed 4 days after hydrodynamic injection. Yac1 lytic ability of hepatic mononuclear cells is expressed as the indicated effector and target ratios (E/T ratio). Experiments were done 3 times and representative data are shown. **e** and **f** GKO mice were intrasplenically injected with CT-26 cells and, 1 day later, intravenously injected with whole mononuclear cells, $DX5^+$ cells or $DX5^-$ cells (4.0×10^6/mouse). Two days after CT-26 injection, mice were hydrodynamically injected with either pCMV-IL-12 or pCMV. **e** The levels of serum IFNγ are expressed as mean and SD (n = 6/group). **f** Fourteen days after plasmid injection, mice were killed to examine liver tumor development by measuring liver weight. The results are expressed as mean and SD (n = 6/group). *ND* not detectable. $^*p < 0.001$

serum levels of IP-10 and MIG, chemokines downstream of IFNγ, were measured after IL-12 therapy (Fig. 6e). pCMV-IL-12-injected mice showed significant increase in both levels compared with pCMV-injected mice. Significant increase after pCMV-IL-12 injection was also found in NK cell-depleted mice, but not in GKO mice. This result suggests that production of these chemokines was not completely suppressed in NK cell-depleted mice in our experimental condition. Immunohistochemical analysis revealed that tumoral accumulation of CD4-positive cells and CD8-positive cells was observed in pCMV-IL-12-injected mice but not in pCMV-injected mice. On the other hand, similar levels of CD31 expression were observed in tumors of pCMV-injected mice and pCMV-IL-12-injected mice (Fig. 6d). These results suggest that IL-12's anti-tumor effects might be mediated by T-cell accumulating in the tumor rather than anti-angiogenesis.

Discussion

IL-12 is recognized as a master regulator of adaptive type 1, cell-mediated immunity. One major action of IL-12 is its induction of other cytokines, particularly IFNγ. A large amount of evidence has indicated that IL-12 administration leads to IFNγ production from a variety of immune cells, such as T cells [16], B cells [17], NK cells [18] and NKT cells [22]. The relative impact of each immune cell as the source of IFNγ has been controversial. The present study highlighted NK cells as a most efficient producer of IFNγ that is critical for IL-12-induced anti-tumor effects.

Flow cytometric analysis revealed higher in vivo production of IFNγ of NK cells than that of other cell types. The levels of serum IFNγ were around fourfold higher in Rag2 KO mice which only possess NK cells than in wild-type mice. On the other hand, NK-cell depletion in wild-type mice led to twofold reduction of serum IFNγ levels. These data indicate substantial contribution of NK cells in IFNγ production in vivo. Previous research has demonstrated that the specific cellular effects of IL-12 are due mainly to activation of STAT4 [23, 24]. IL-12-induced STAT4 phosphorylation leads to the production of IFNγ [25]. In agreement with these reports, our in vitro analysis showed that, in contrast to STAT1, STAT4 was directly phosphorylated upon IL-12 stimulation, being independent of IFNγ. Of interest is the finding that NK cells express higher levels of STAT4 than non-NK cells, suggesting that NK cells possess an ideal expression profile of STATs for producing IFNγ upon IL-12 stimulation. Indeed, in vitro analysis revealed that NK cells, upon IL-12 exposure, displayed higher levels of IFNγ production as well as STAT4 phosphorylation than non-NK cells. These in vitro

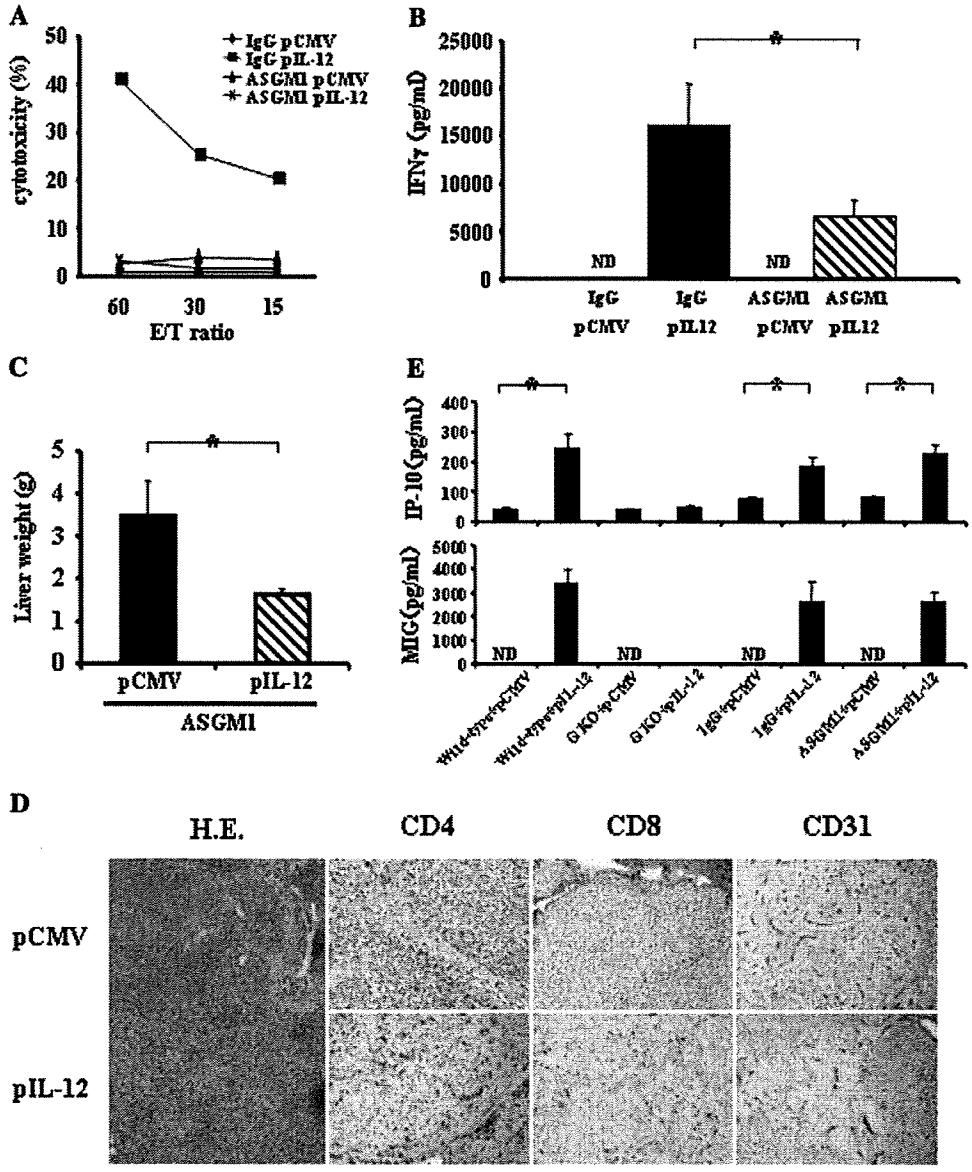

Fig. 6 Anti-tumor effects of IL-12 in NK-cell-depleted mice. Serum IFNγ levels and NK-cell activation. Wild-type mice were intraperitoneally injected with either anti-asialoGM1 antibody (ASGM1) or control IgG, and, 1 day later hydrodynamically injected with either pCMV-IL-12 or pCMV. Mice were killed 4 days after plasmid injection. **a** Yac1 lytic ability of hepatic mononuclear cells is expressed as the indicated effector and target ratios (E/T ratio). Experiments were done 2 times and representative data are shown. **b** The levels of serum IFNγ are expressed as mean and SD ($n = 6$/group). *ND* not detectable. *$p < 0.005$. Anti-metastatic effects. Wild-type mice were intrasplenically injected with CT-26 cells and, 1 day later and then every 5 days, intraperitoneally injected with either anti-asialoGM1 antibody (ASGM1) or control IgG, and hydrodynamically injected with either pCMV-IL-12 or pCMV 2 days after CT-26 injection. Fourteen days after plasmid injection, mice were killed to examine liver tumor development by measuring liver weight. **c** The results are indicated as mean and SD ($n = 6$/group). *$p < 0.001$. **d** Representative histology of liver sections analyzed by hematoxylin-eosin staining and immunohistochemistry of CD4, CD8 and CD31. **e** Serum levels of IP-10 and MIG. Wild-type or GKO mice were hydrodynamically injected with either pCMV-IL-12 or pCMV. Wild-type mice were intraperitoneally injected with either anti-asialoGM1 antibody (ASGM1) or control IgG, and 1 day later hydrodynamically injected with either pCMV-IL-12 or pCMV. Four days later, each mice were bled to measure the levels of serum IP-10 and MIG. Results are expressed as mean and SD ($n = 6$/group). *ND* not detectable. *$p < 0.001$

data are consistent with the in vivo observation that NK cells are efficient producers of IFNγ during IL-12 therapy.

Many studies have demonstrated that IFNγ production is required for the anti-tumor effects of IL-12 [14, 26, 27]. In fact, we have demonstrated that deletion of IFNγ abolished NK cytotoxicity and the anti-metastatic effect of IL-12 therapy in the liver. A large amount of evidence supports the concept that a major action of IL-12 is to promote the differentiation of naïve CD4 + T cells into Th1 cells, which produce IFNγ. Previous research reported that CD4

T-cell depletion caused inhibition of anti-tumor effects. More recent studies have supported a critical role of IFNγ as a third signal for CD8 T-cell differentiation. There have been many reports focusing on IFNγ production from T cells induced by IL-12 for the anti-tumor effect of IL-12 [28]. Segal et al. performed an elegant study showing a critical role of T-cell production of IFNγ in the anti-tumor effect by adoptively transferring T cells into GKO mice in a subcutaneous tumor model [29]. However, apart from this study, little is known about the contribution of each immune cell as a producer of IFNγ in terms of an anti-tumor effect. In our model, T-cell mediated adaptive responses were not required for the anti-metastatic effect of IL-12. More importantly, the anti-metastatic effects of IL-12 were restored in GKO mice by an adoptive transfer of wild-type NK cells. The same number of non-NK cells could not provoke IL-12-induced anti-tumor effects in GKO mice. The present study demonstrated for the first time a potent effect of NK cells on producing IFNγ that was critical for anti-metastatic effect during IL-12 therapy.

Our study showed that the main IFNγ producer of IL-12 was NK cells. So we focused on NK cells which were activated by IL-12 in an IFNγ-dependent manner to examine the cellular mechanism of protection against hepatic metastasis. Many studies have shown the importance of each subset (NK- [12], NKT- [10] and T [9, 30] cells) for anti-tumor effects of IL-12. In the present study, NK cells were sufficient while T cells, B cells, NKT cells were dispensable for IL-12-mediated NK-cell activation and anti-metastatic effects as IL-12 therapy showed Yac1 lytic ability and antimetastatic effects in Rag2 KO mice. On the other hand, NK-cell depletion by a repeated injection of anti-aialoGM1 antibody protected wild-type mice from macroscopic liver metastasis, but did not from microscopic liver metastasis. Thus, although NK cells were required for a full-blown IL-12 anti-tumor effect, other anti-tumor pathways are activated by IL-12 in the absence of NK cells. Serum levels of IP-10 and MIG suggest that production of these chemokines downstream of IFNγ was not suppressed in NK-cell-depleted mice in our experimental condition. When compared with the experiment on GKO mice, accumulation of CD4-positive cells and CD8-positive cells were more evident in NK-cell-depleted mice than in GKO mice (Supplementary Figure). On the other hand, there was no remarkable difference in the expression of CD31 between pCMV injection and pCMV-IL-12 injection. These results suggested that in NK-cell-depleted mice IL-12 may exert anti-tumor effect via T-cell accumulation rather than anti-angiogenesis.

Since the liver contains an abundance of immune cells (especially NK cells) [31], the cytokine-mediated activation of these cells may be a promising approach toward anti-tumor therapy in this organ [32]. IL-12 is a cytokine known to elicit a potent anti-tumor effect in mouse experimental models. However, clinical trials attempted to date were interrupted by fatal adverse effects. Systemic IL-12 therapy has been associated with dose-limiting toxicity [33]. IL-12 induces activation of the pro-inflammatory pathway which causes the complications of high dose cytokine, independent of the action of IFNγ [34]. On the other hand, the levels of immunosuppressive cytokine, for example, TGF-β1 or IL-10 were significantly higher in patients with hepatocellular cancer and colon cancer [35–38]. In particular, TGF-β1 in serum can limit NK-cell IFNγ production [39]. Thus, in patients with advanced disease, IL-12 may not be able to exert its potent anti-tumor immune-effects because IFNγ, which is an important mediator of the IL-12-induced immune response, is less effective in a tumor environment. In the present study, we demonstrated that NK-cell IFNγ production induced by IL-12 was sufficient for the anti-metastatic effect of IL-12 in the liver. Thus, a strategy of efficiently producing IFNγ from NK cells may be important for avoiding toxicity of IL-12 therapy.

IL-12 gene therapy has an advantage to allow local production of the cytokine at the tumor sites with low serum concentration. Studies demonstrated that intratumoral administration of adenovirus encoding IL-12 to animals with different types of carcinoma caused complete tumor eradication and increased long-term survival [40, 41]. Moreover, injection of IL-12-encoding adenovirus in one nodule of liver tumor resulted in regression of distant nodules in the liver [41]. However, in a clinical trial anti-tumor activity of IL-12-encoding adenovirus was only observed in the injected tumor sites, but not in distant tumors [42]. The present study shed light on hydrodynamic transfection of hepatocytes as a promising strategy to eradicate disseminated tumors from whole liver.

In summary, NK cells are not just an effector for innate immunity but a mediator producing IFNγ that is critical for the IL-12 anti-tumor effects. Extremely higher expression of STAT4 may be a basis for efficient production of IFNγ from NK cells.

Acknowledgments We thank Dr. Morihiro Watanabe (Laboratory of Experimental Immunology, Division of Basic Sciences, National Cancer Institute-Frederick Cancer Research and Development Center) for providing the pCMV-IL-12 plasmid, Dr. Yoichiro Iwakura (University of Tokyo, Institute of Medical Science) for providing GKO mice.

References

1. Kobayashi M, Fitz L, Ryan M, Hewick RM, Clark SC, Chan S, Loudon R, Sherman F, Perussia B, Trinchieri G (1989) Identification and purification of natural killer cell stimulatory factor

(NKSF), a cytokine with multiple biologic effects on human lymphocytes. J Exp Med 170(3):827–845
2. Stern AS, Podlaski FJ, Hulmes JD, Pan YC, Quinn PM, Wolitzky AG, Familletti PC, Stremlo DL, Truitt T, Chizzonite R, Gately MK (1990) Purification to homogeneity and partial characterization of cytotoxic lymphocyte maturation factor from human B-lymphoblastoid cells. Proc Natl Acad Sci USA 87(17):6808–6812
3. Watford WT, Moriguchi M, Morinobu A, O'Shea JJ (2003) The biology of IL-12: coordinating innate and adaptive immune responses. Cytokine Growth Factor Rev 14(5):361–368
4. Trinchieri G (2003) Interleukin-12 and the regulation of innate resistance and adaptive immunity. Nat Rev Immunol 3(2):133–146
5. Colombo MP, Trinchieri G (2002) Interleukin-12 in anti-tumor immunity and immunotherapy. Cytokine Growth Factor Rev 13(2):155–168
6. Del Vecchio M, Bajetta E, Canova S, Lotze MT, Wesa A, Parmiani G, Anichini A (2007) Interleukin-12: biological properties and clinical application. Clin Cancer Res 13(16):4677–4685
7. Wigginton JM, Gruys E, Geiselhart L, Subleski J, Komschlies KL, Park JW, Wiltrout TA, Nagashima K, Back TC, Wiltrout RH (2001) IFN-gamma and Fas/FasL are required for the antitumor and antiangiogenic effects of IL-12/pulse IL-2 therapy. J Clin Invest 108(1):51–62
8. Lee JC, Kim DC, Gee MS, Saunders HM, Sehgal CM, Feldman MD, Ross SR, Lee WM (2002) Interleukin-12 inhibits angiogenesis and growth of transplanted but not in situ mouse mammary tumor virus-induced mammary carcinomas. Cancer Res 62(3):747–755
9. Brunda MJ, Luistro L, Warrier RR, Wright RB, Hubbard BR, Murphy M, Wolf SF, Gately MK (1993) Antitumor and antimetastatic activity of interleukin 12 against murine tumors. J Exp Med 178(4):1223–1230
10. Cui J, Shin T, Kawano T, Sato H, Kondo E, Toura I, Kaneko Y, Koseki H, Kanno M, Taniguchi M (1997) Requirement for Valpha14 NKT cells in IL-12-mediated rejection of tumors. Science 278(5343):1623–1626
11. Zilocchi C, Stoppacciaro A, Chiodoni C, Parenza M, Terrazzini N, Colombo MP (1998) Interferon gamma-independent rejection of interleukin 12-transduced carcinoma cells requires CD4 + T cells and Granulocyte/Macrophage colony-stimulating factor. J Exp Med 188(1):133–143
12. Kodama T, Takeda K, Shimozato O, Hayakawa Y, Atsuta M, Kobayashi K, Ito M, Yagita H, Okumura K (1999) Perforin-dependent NK cell cytotoxicity is sufficient for anti-metastatic effect of IL-12. Eur J Immunol 29(4):1390–1396
13. Takeda K, Hayakawa Y, Atsuta M, Hong S, Van Kaer L, Kobayashi K, Ito M, Yagita H, Okumura K (2000) Relative contribution of NK and NKT cells to the anti-metastatic activities of IL-12. Int Immunol 12(6):909–914
14. Ogawa M, Yu WG, Umehara K, Iwasaki M, Wijesuriya R, Tsujimura T, Kubo T, Fujiwara H, Hamaoka T (1998) Multiple roles of interferon-gamma in the mediation of interleukin 12-induced tumor regression. Cancer Res 58(11):2426–2432
15. Subleski JJ, Hall VL, Back TC, Ortaldo JR, Wiltrout RH (2006) Enhanced antitumor response by divergent modulation of natural killer and natural killer T cells in the liver. Cancer Res 66(22):11005–11012
16. Kubin M, Kamoun M, Trinchieri G (1994) Interleukin 12 synergizes with B7/CD28 interaction in inducing efficient proliferation and cytokine production of human T cells. J Exp Med 180(1):211–222
17. Yoshimoto T, Okamura H, Tagawa YI, Iwakura Y, Nakanishi K (1997) Interleukin 18 together with interleukin 12 inhibits IgE production by induction of interferon-gamma production from activated B cells. Proc Natl Acad Sci USA 94(8):3948–3953
18. Lauwerys BR, Renauld JC, Houssiau FA (1999) Synergistic proliferation and activation of natural killer cells by interleukin 12 and interleukin 18. Cytokine 11(11):822–830
19. Takehara T, Uemura A, Tatsumi T, Suzuki T, Kimura R, Shiotani A, Ohkawa K, Kanto T, Hiramatsu N, Hayashi N (2007) Natural killer cell-mediated ablation of metastatic liver tumors by hydrodynamic injection of IFNalpha gene to mice. Int J Cancer 120(6):1252–1260
20. Watanabe M, Fenton RG, Wigginton JM, McCormick KL, Volker KM, Fogler WE, Roessler PG, Wiltrout RH (1999) Intradermal delivery of IL-12 naked DNA induces systemic NK cell activation and Th1 response in vivo that is independent of endogenous IL-12 production. J Immunol 163(4):1943–1950
21. Takehara T, Suzuki T, Ohkawa K, Hosui A, Jinushi M, Miyagi T, Tatsumi T, Kanazawa Y, Hayashi N (2006) Viral covalently closed circular DNA in a non-transgenic mouse model for chronic hepatitis B virus replication. J Hepatol 44(2):267–274
22. Shin T, Nakayama T, Akutsu Y, Motohashi S, Shibata Y, Harada M, Kamada N, Shimizu C, Shimizu E, Saito T, Ochiai T, Taniguchi M (2001) Inhibition of tumor metastasis by adoptive transfer of IL-12-activated Valpha14 NKT cells. Int J Cancer 91(4):523–528
23. Thierfelder WE, van Deursen JM, Yamamoto K, Tripp RA, Sarawar SR, Carson RT, Sangster MY, Vignali DA, Doherty PC, Grosveld GC, Ihle JN (1996) Requirement for Stat4 in interleukin-12-mediated responses of natural killer and T cells. Nature 382(6587):171–174
24. Kaplan MH, Sun YL, Hoey T, Grusby MJ (1996) Impaired IL-12 responses and enhanced development of Th2 cells in Stat4-deficient mice. Nature 382(6587):174–177
25. Morinobu A, Gadina M, Strober W, Visconti R, Fornace A, Montagna C, Feldman GM, Nishikomori R, O'Shea JJ (2002) STAT4 serine phosphorylation is critical for IL-12-induced IFN-gamma production but not for cell proliferation. Proc Natl Acad Sci USA 99(19):12281–12286
26. Comes A, Di Carlo E, Musiani P, Rosso O, Meazza R, Chiodoni C, Colombo MP, Ferrini S (2002) IFN-gamma-independent synergistic effects of IL-12 and IL-15 induce anti-tumor immune responses in syngeneic mice. Eur J Immunol 32(7):1914–1923
27. Hafner M, Falk W, Echtenacher B, Mannel DN (1999) Interleukin-12 activates NK cells for IFN-gamma-dependent and NKT cells for IFN-gamma-independent antimetastatic activity. Eur Cytokine Netw 10(4):541–548
28. Komita H, Homma S, Saotome H, Zeniya M, Ohno T, Toda G (2006) Interferon-gamma produced by interleukin-12-activated tumor infiltrating CD8 + T cells directly induces apoptosis of mouse hepatocellular carcinoma. J Hepatol 45(5):662–672
29. Segal JG, Lee NC, Tsung YL, Norton JA, Tsung K (2002) The role of IFN-gamma in rejection of established tumors by IL-12: source of production and target. Cancer Res 62(16):4696–4703
30. Nastala CL, Edington HD, McKinney TG, Tahara H, Nalesnik MA, Brunda MJ, Gately MK, Wolf SF, Schreiber RD, Storkus WJ, Lotze MT (1994) Recombinant IL-12 administration induces tumor regression in association with IFN-gamma production. J Immunol 153(4):1697–1706
31. Doherty DG, O'Farrelly C (2000) Innate and adaptive lymphoid cells in the human liver. Immunol Rev 174:5–20
32. Seki S, Habu Y, Kawamura T, Takeda K, Dobashi H, Ohkawa T, Hiraide H (2000) The liver as a crucial organ in the first line of host defense: the roles of Kupffer cells, natural killer (NK) cells and NK1.1 Ag + T cells in T helper 1 immune responses. Immunol Rev 174:35–46
33. Car BD, Eng VM, Lipman JM, Anderson TD (1999) The toxicology of interleukin-12: a review. Toxicol Pathol 27(1):58–63
34. Biber JL, Jabbour S, Parihar R, Dierksheide J, Hu Y, Baumann H, Bouchard P, Caligiuri MA, Carson W (2002) Administration of

two macrophage-derived interferon-gamma-inducing factors (IL-12 and IL-15) induces a lethal systemic inflammatory response in mice that is dependent on natural killer cells but does not require interferon-gamma. Cell Immunol 216(1–2):31–42
35. Tsushima H, Ito N, Tamura S, Matsuda Y, Inada M, Yabuuchi I, Imai Y, Nagashima R, Misawa H, Takeda H, Matsuzawa Y, Kawata S (2001) Circulating transforming growth factor beta 1 as a predictor of liver metastasis after resection in colorectal cancer. Clin Cancer Res 7(5):1258–1262
36. Okumoto K, Hattori E, Tamura K, Kiso S, Watanabe H, Saito K, Saito T, Togashi H, Kawata S (2004) Possible contribution of circulating transforming growth factor-beta1 to immunity and prognosis in unresectable hepatocellular carcinoma. Liver Int 24(1):21–28
37. Chau GY, Wu CW, Lui WY, Chang TJ, Kao HL, Wu LH, King KL, Loong CC, Hsia CY, Chi CW (2000) Serum interleukin-10 but not interleukin-6 is related to clinical outcome in patients with resectable hepatocellular carcinoma. Ann Surg 231(4):552–558
38. Galizia G, Lieto E, De Vita F, Romano C, Orditura M, Castellano P, Imperatore V, Infusino S, Catalano G, Pignatelli C (2002) Circulating levels of interleukin-10 and interleukin-6 in gastric and colon cancer patients before and after surgery: relationship with radicality and outcome. J Interferon Cytokine Res 22(4):473–482
39. Meadows SK, Eriksson M, Barber A, Sentman CL (2006) Human NK cell IFN-gamma production is regulated by endogenous TGF-beta. Int Immunopharmacol 6(6):1020–1028
40. Caruso M, Pham-Nguyen K, Kwong YL, Xu B, Kosai KI, Finegold M, Woo SL, Chen SH (1996) Adenovirus-mediated interleukin-12 gene therapy for metastatic colon carcinoma. Proc Natl Acad Sci USA 93(21):11302–11306
41. Barajas M, Mazzolini G, Genove G, Bilbao R, Narvaiza I, Schmitz V, Sangro B, Melero I, Qian C, Prieto J (2001) Gene therapy of orthotopic hepatocellular carcinoma in rats using adenovirus coding for interleukin 12. Hepatology 33(1):52–61
42. Sangro B, Mazzolini G, Ruiz J, Herraiz M, Quiroga J, Herrero I, Benito A, Larrache J, Pueyo J, Subtil JC, Olague C, Sola J et al (2004) Phase I trial of intratumoral injection of an adenovirus encoding interleukin-12 for advanced digestive tumors. J Clin Oncol 22(8):1389–1397

Cancer Immunol Immunother
DOI 10.1007/s00262-009-0796-2

ORIGINAL ARTICLE

EphA2-derived peptide vaccine with amphiphilic poly(γ-glutamic acid) nanoparticles elicits an anti-tumor effect against mouse liver tumor

Shinjiro Yamaguchi · Tomohide Tatsumi · Tetsuo Takehara · Akira Sasakawa · Masashi Yamamoto · Keisuke Kohga · Takuya Miyagi · Tatsuya Kanto · Naoki Hiramastu · Takami Akagi · Mitsuru Akashi · Norio Hayashi

Received: 21 August 2009 / Accepted: 10 November 2009

Abstract The prognosis of liver cancer remains poor, but recent advances in nanotechnology offer promising possibilities for cancer treatment. Novel adjuvant, amphiphilic nanoparticles (NPs) composed of L-phenylalanine (Phe)-conjugated poly(γ-glutamic acid) (γ-PGA-Phe NPs) having excellent capacity for carrying peptides, were found to have the potential for use as a peptide vaccine against tumor models overexpressing artificial antigens, such as ovalbumin (OVA). However, the anti-tumor potential of γ-PGA-Phe NPs vaccines using much less immunogenic tumor-associated antigen (TAA)-derived peptide needs to be clarified. In this study, we evaluated the effectiveness of immunization with EphA2, recently identified TAA, derived peptide-immobilized γ-PGA-Phe NPs (Eph-NPs) against mouse liver tumor of MC38 cells (EphA2-positive colon cancer cells). Immunization of normal mice with Eph-NPs resulted in generation of EphA2-specific type-1 CD8+ T cells. Immunization with Eph-NPs tended to provide a degree of anti-MC38 liver tumor protection more than that observed for immunization with the mixture of EphA2-derived peptide and complete Freund's adjuvant (Eph + CFA). Neither Eph-NPs nor Eph + CFA vaccines inhibited tumor growth of BL6, EphA2-negative melanoma cells. Splenocytes isolated from MC38-bearing mice treated with Eph-NPs showed strong and specific cytotoxic activity against MC38 cells. Immunization with Eph + CFA induced liver damage as evidenced by elevation of serum alanine aminotransferase, while Eph-NPs vaccination did not exhibit any toxic damage to the liver. These results demonstrated that immunization with Eph-NPs displayed anti-tumor effects against liver tumor by generating acquired immunity equivalent to the toxic adjuvant CFA, suggesting that safe γ-PGA-Phe NPs could be applied clinically for the vaccine treatment of liver cancer.

Keywords Peptide vaccine · EphA2-derived peptide · Acquired immunity · Liver tumor

Abbreviations

IFA	Incomplete Freund's adjuvant
NPs	Nanoparticles
γ-PGA	Poly(γ-glutamic acid)
Phe	L-Phenylalanine
CFA	Complete Freund's adjuvant
PBS	Phosphate buffered saline
i.p.	Intraperitoneal
ALT	Alanine aminotransferase
DCs	Dendritic cells

Introduction

Immunotherapies using peptide vaccine combined with immunologic adjuvants, such as incomplete Freund's

S. Yamaguchi and T. Tatsumi contributed equally to this work.

S. Yamaguchi · T. Tatsumi (✉) · T. Takehara · A. Sasakawa · M. Yamamoto · K. Kohga · T. Miyagi · T. Kanto · N. Hiramastu · N. Hayashi
Department of Gastroenterology and Hepatology, Osaka University Graduate School of Medicine, 2-2 Yamadaoka, Suita, Osaka 565-0871, Japan
e-mail: tatsumit@gh.med.osaka-u.ac.jp

T. Akagi · M. Akashi
Department of Applied Chemistry, Graduate School of Engineering, Osaka University, Suita, Japan

S. Yamaguchi · T. Tatsumi · T. Takehara · A. Sasakawa · M. Yamamoto · T. Akagi · M. Akashi · N. Hayashi
Core Research for Evolutional Science and Technology (CREST), Japan Science and Technology Agency (JST), Tokyo, Japan

Published online: 27 November 2009